# Politecnico di Torino

Master Degree in Environmental and Land Engineering
Climate Change

# Experimental Test on Passive Seismic Methods for the Monitoring of Embankments

**Candidate:**          Farzane Attari

**Supervisor:**          Prof. Chiara Colombero

**Co-supervisors:**       Prof. Alberto Godio
                         Valeria strallo

**March 2025**

# Summary

Earthen embankments are important structures in Alpine regions, their characterization and continuous monitoring is necessary in order to verify their stability and integrity over time. This aspect has such a vital role in these areas, as the economy and social community has a strong dependence on the stability of embankments. Although there are lots of studies conducting with ERT or active seismic monitoring of the embankment, there are lack of such studies to continuous monitoring and characterization of earthen embankments particularly in Alpine regions. Hence, the aim of this study is to conduct a continuous monitoring and characterization of an earthen embankment for a short period of time from July 2023 to May 2024 with passive seismic investigation. The selected site is Fourcare embankment located in Aosta Valley northwest of Italy built by Monterosa Company to support water needed for snow production of the Larici ski resort.

Passive seismic geophysical method was chosen as it is non-invasive, cost-effective, and allows for continuous data collection. Passive seismic method uses ambient seismic noise without the need to have the active source to create the artificial wave. In this case, we had the data from four passive seismic monitoring stations at Fourcare embankment along with meteorological data from the nearest meteorological station to the embankment. The method performed Power Spectral Density Analysis verified that the ambient noise falls within the Peterson's New Noise Model and New High Noise Model. Following that the Ambient Seismic Noise Spectral Analysis was performed which characterized the resonance frequency of the embankment body around 10 Hz which was almost stable over time. Additionally, microseismicity analysis was performed that detect microseismic events with the STA/LTA algorithm. After event detection, classification was done by visual interpretation, and three main categories were identified. The first category has the characteristic of low frequency and short time duration which potentially is associated with the propagation of the fractures in the embankment structure. And the second one is characterized by the same frequency close to 10 Hz but longer duration almost a horizontal spectrogram which appears mostly in winter period likely related to the sliding due to water infiltration. And the third category has a characteristic of the longer frequency around 40 Hz with

longer duration which is likely related to snow compaction or freezing in shallower layers. Furthermore, the cumulative number of events was shown and analyse its response to temperature which shows that there is when temperature drops around October the number of microseismic events increased. Finally, the scatter plot of the frequency of events was done. The peak frequency of events reveals that the microseismic events are mainly scattered around two distinct frequencies. Moreover, it shows that the combination of temperature drop, and precipitation can aggregate the peak of frequencies around these two frequencies. This study shows that there can be done further studies to continuous monitoring of embankments even for longer periods of time.

# Acknowledgment

I would like to thanks to my professor, Chiara Colombero, whose sincere support has guided me throughout this journey. I would also like to thank my family for their constant encouragement and presence as well as my friends, and above all, Mohamad, who has always been a source of guidance whenever I needed it.

My heartful thanks to the greatest teacher of my life, my father who always lights my path. His memory is with me every day and inspires me.

# Contents

# List of Figures

# Chapter 1

# Introduction

Throughout history, embankments have assumed a critical position in the growth and formation of human settlements and urban development. These structures have different purposes, from flood protection to enhancing urban aesthetics, which in turn determines their social dynamics and economic activities. An embankment is a structure used to impound water and form reservoirs. These structures are either the result of human activities or natural phenomena, such as landslides or glacier deposits (United States Bureau of Reclamation, 1987).

Those embankment dams that are built mainly by natural materials, such as compacted soil or rock material which were excavated from the nearby of the site are referred to as earthen embankment. The structural integrity of embankment dams depends on the compression of the materials and proper layering; however, the degree of compaction is different according to different construction methods used. Thus, the construction and performance of earthen embankments are highly reliant on the materials and techniques used (Regis Neroni, Kevin Stephens, & Daniel Dwumfour, 2019)

Earthen embankments are widely used as water-impounding structures to harvest and divert water for usages such as supplemental irrigation, hydropower generation, flood protection and river course modification. These structures might also function as fences barriers to keep rivers from overflowing their banks and nearby lands; thus, protecting communities and agricultural areas. Additionally, embankments can modify river courses by diverting water into channels, tunnels, or artificial reservoirs. These are not only useful in fulfilling the needs for irrigation and water supply, but also for recreational purposes (Singh, 2023).

Despite large embankments, small embankments are also crucial. They constitute many structures (over 800,000 worldwide), often they are not as highly regarded as the larger embankments. Many of them were built many years ago when the regulations and standards were not strict and even most of them are constructed near populated areas. These small embankments have a greater likelihood of failure

than larger ones, making them eligible for improved oversight and maintenance (Fantilli, De Biagi, Veylon , & Frigo, 2017); (K. Brewitt & L. M. Colwyn, 2019).

Small embankments also have a significant impact on local hydrology and water quality of the immediate area by changing dynamics of the flow, transport of nutrient, and ecological integrity of the water course. These structures can restrict stream flows, as a result altering the level of dissolved oxygen, which can lead to fluctuations in the quality of water. Furthermore, environmental stresses such as heavy rainfall, poor drainage, seismic activity, high water content, steep slopes, and improper compaction can exert additional forces on embankments. Hence, careful design and continuous monitoring are pivotal to mitigate potential negative effects and ensure long-term stability (Morden, Horne, Bond, Nathan, & Olden, 2022).

Earthen embankments are prone to several types of failures due to material properties, inadequate maintenance, or operational practices. The key failure mechanisms are identified as internal erosion, pore overpressures, and structural deformation. Another type of failure can happen when water overtops the height of the embankment and creates erosion and eventually leading to the collapse of the embankment. This process called overtopping. Insufficient freeboard or inadequate design parameters often contribute to this failure. The phenomenon is an erosion of particles by water that is flowing through the pore space of the embankment and a progressive creation of channels inside the structure. This process weakens the embankment, leading to potential collapse. Among the possible failure mechanisms, internal erosion is rather challenging to recognize with traditional screening or monitoring techniques. (Foster, Fell, & Spannagle, 2000).

Figure 1 illustrates the occurrence of internal erosion in an earthen embankment dam and its impact on a downstream town. Embankment safety and functionality cannot be ensured without proper monitoring and maintenance. Many new and innovative methods are available which improve the traditional methods of monitoring. These methods include passive seismic techniques, remote sensing technologies, electrical resistivity tomography, automated frameworks, and UAV photogrammetry (Thomas, et al., 2024).
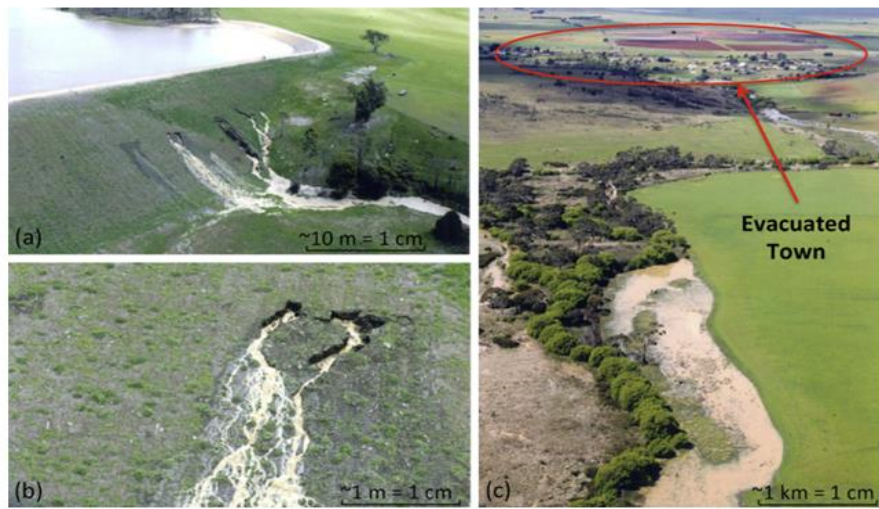
**Figure 1 - The photos show (a) the failure of the Tunbridge earthfill dam in Tasmania, Australia due to internal erosion, with (b) a portion of seepage from dam and (c) a close-up view of the evacuated town in downstream. source: Jeffery Farrar (2008)**



**Figure 2 - The Fourcare Embankment in the Aosta Valley was built by Monterosa Ski Resort in 2019 on Bettaforca in the Italian Alps.**

# Chapter 2

# Methods

## 2.1 Test Site Description

### 2.1.1 Alpine Ski Resorts and Climate Change

Alpine ski resorts are important economically and culturally. They attract millions of visitors annually with their breathtaking snowy landscapes. Alpine resorts depend on natural snowfall to sustain skiing, snowboarding, and related activities, which have a significant contribution to the local economy. However, climate change with disruption of snowfall patterns and reduction of the duration of snow seasons pose significant challenges on the sustainability of these structures. Rising temperatures and sparse precipitation have more complicated the predictability of snowfall (Steiger & Mayer, 2008). Snowmaking is used to mitigate these challenges and to ensure the expansion of the operational season, even during periods of reduced snowfall. Nevertheless, as snowmaking is water-intensive activity, there is a need to store water; hence, the construction of reservoirs, often in the form of earthen embankments (Rixen, et al., 2011).

In the Fourcare site, 95,000 cubic meters was excavated, to create the bed of the water basin. The maximum excavation depth was 11.50 meters. Then a lining material (fine material 20-30 cm) was used to cover the bed. Additionally, using an impermeable membrane as well as two non-woven fabric layers to ensure the waterproofing of the embankment's bottom and prevention of further leakage. Following the compaction of the embankment bed, a drainage system was built to collect the groundwater and the intercepted water, and direct to a manoeuvring pond in order to be used again by a pumping system. Specifically, there was an effort to design of the morphology of the shores in order to neutralize the water basin's appearance. Special stones were added to the top part of the shores to ensure the environmental integration of the structure. Figure 3 shows the Fourcare embankment cross-section.

## 2.1.2 The Study Site: Fourcare Artificial Basin (Aosta Valley, NW Italy)

The Fourcare artificial water basin is located in the Aosta Valley, in north-western Italy, built by Monterosa S.p.A. The energy projects are the main focus of Monterosa S.p.A., and it mainly deals with the management of snow and water reservoirs, which are important for both energy supply and other related tourism activities such as skiing. The Fourcare embankment which is designed to supply snow to the nearby ski resorts (Larici ski slope) is a part of a larger network of hydroelectric plants in the area. It is located at an altitude of 2,332 meters above sea level, built in the 1990s and has a capacity of 127,120 cubic meters of water. This embankment is critical in managing snow production of the region. Figure 2 shows the Fourcare Embankment, constructed in the Aosta Valley by Monterosa Ski Resort in 2019.

The Fourcare embankment was created in accordance with the principles of the Italian regulatory frameworks such as Decree of the Ministry of Infrastructure and Transport (2014) and the 2018 Technical Standards for Construction (NTC 2018). Fourcare embankment address broader environmental and energy concerns in apart from its critical importance in terms of local tourism. Its role highlights the strong connection of infrastructure, environmental management, and economic stability in alpine regions. Figure 5 presents the planimetric view of the Fourcare Embankment.

Furthermore, there are seven piezometers around the Fourcare embankment in order to measure the water table level. Figure 4 Shows the result of the measurement from these seven piezometers from November 2018 to January 2023. as the piezometer number 8 has the highest water table level which means shallowest depth to the groundwater at approximately 2 meters, and the piezometer number 10 measures the lowest water table level among all the piezometers. The value measured by the piezometer number 10 is more or less 13 meters which indicates the deepest level to reach the groundwater within the Fourcare embankment is around 13 meters. These results illustrate that the hydraulic head direction of the water table level in the Fourcare embankment is likely from the North-East to South.
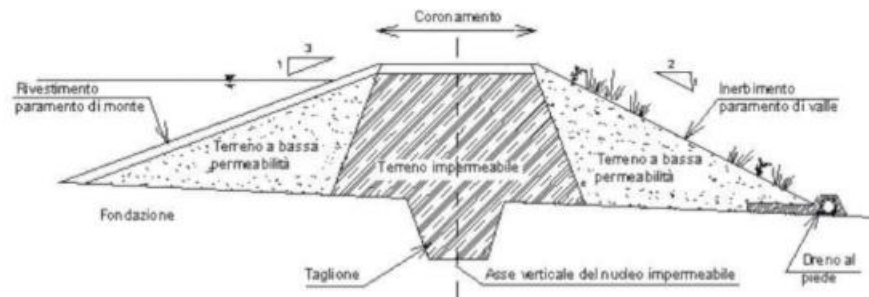
**Figure 3 - shows the Fourcare embankment cross-section.**
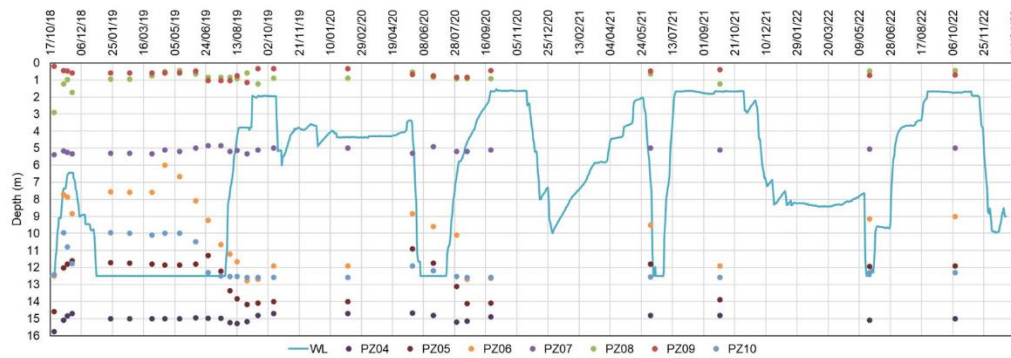


**Figure 4 - shows the results of piezometers around the Fourcare embankment from November 2018 to January 2023.**
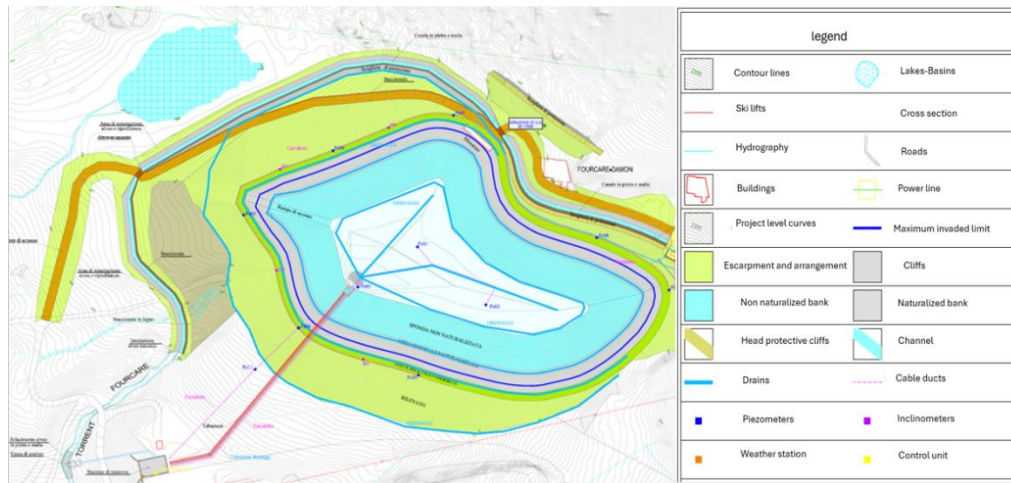
**Figure 5 - Fourcare Embankment in Aosta Valley, by Monterosa company**



**Figure 6 - shows the position of four passive seismic monitoring stations at the Fourcare Embankment; the four red square from 1 to 4 represent the passive seismic monitoring stations while the points (i) show the positions of inclinometers and (pz) are the piezometers.**

Additional to piezometric data, the measurements from inclinometers installed around the Fourcare embankment is available. Inclinometers is a pipe in which there are two perpendicular guides as well as a prob to see if the pipe remains vertical or it has some sort of shifts or movements due to the instability of the embankment. If in the records of inclinometers there is no displacement and profile change is close to zero in the order of millimeters; therefore, the embankment body is stable.

In the Fourcare site, there are four inclinometers which monitor any displacement by a prob with two perpendicular axes A and B moving along the borehole from March 2019 to June 2023, which is depicted in Figure 7, Figure 8, Figure 9, and Figure 10. In Figure 7, and Figure 10, as it can be seen there is no detection of instability at the inclinometer number 1 and 4, respectively. While there is a slight deformation in the data recorded at the inclinometer number 2 at the depth of 5.5 to 8 meters in both directions of the inclinometer's guides, indicating some small displacement as shown in Figure 8.

However, the most distortion happens in inclinometer number four at the depth of 6 to 12 meters which is located in the northern part of the site, which can be an indication of weakening material and possible instability of the embankment structure. Moreover, the presence of a lake that seems has a natural origin on the North side of the embankment as shown in the Figure 5, potentially may have influence on the integrity of the embankment body. Likely, there might be a connection between the water leakages from the Fourcare embankment to the water of the lake.

Because of the displacement recorded in the inclinometer and the presence of the lake on this section of the site that might have a potential connection with water leakage of the artificial embankment, it has been decided to install the four passive seismic monitoring stations in this section of the site to ensure a continuous monitoring and evaluation of the stability of the most critical area of the Fourcare embankment.

### 2.1.3 Aim

This thesis investigates monitoring and maintenance challenges of an earthen embankment in an alpine environment by the application of geophysical techniques, specifically passive seismic analysis. The performance of the basin is essential for the ski resort, as structural failure or hidden seepage can significantly impact snow production, thereby impacting the local economy. The passive seismic methods provide a non-invasive, time saving and cost-effective approach to continuously monitor the embankments and improve the understanding of their hydrodynamic processes. This research aims to detect resonance frequencies, providing insights into internal structural conditions, and identify fractures or permeable zones that may act as pathways for water infiltration.
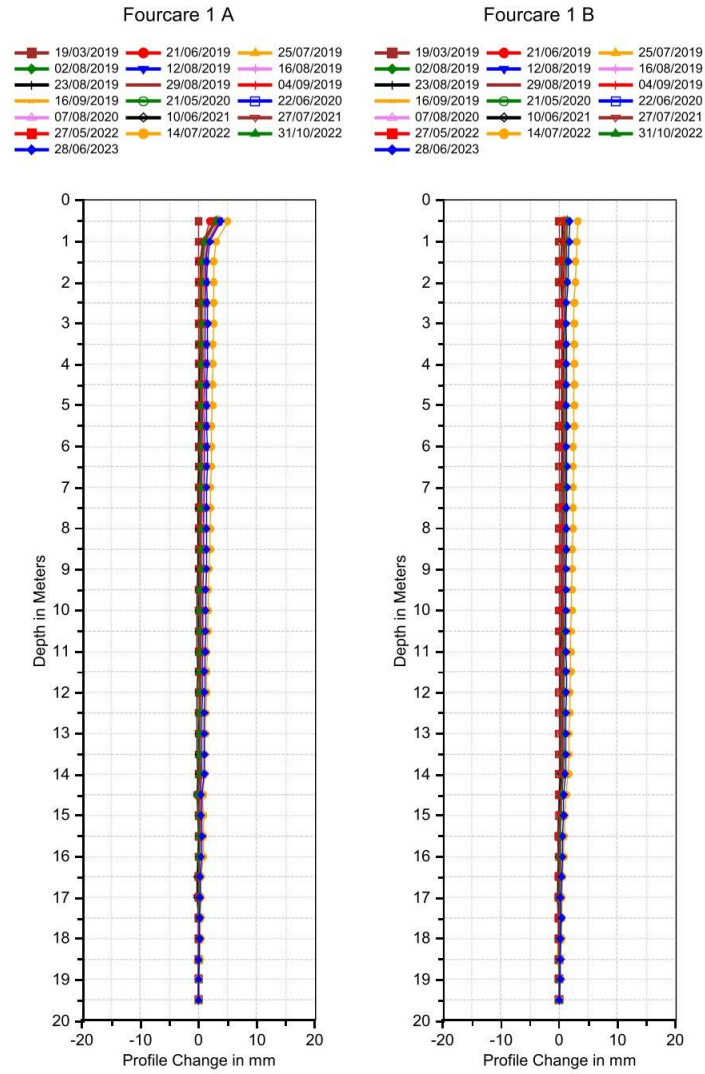
**Figure 7 - shows the displacement profile recorded at inclinometer number 1 around the Fourcare embankment. It represents the distortion along the primary axis (A) of the probe and the lateral axis (B), which is perpendicular to axis A.**
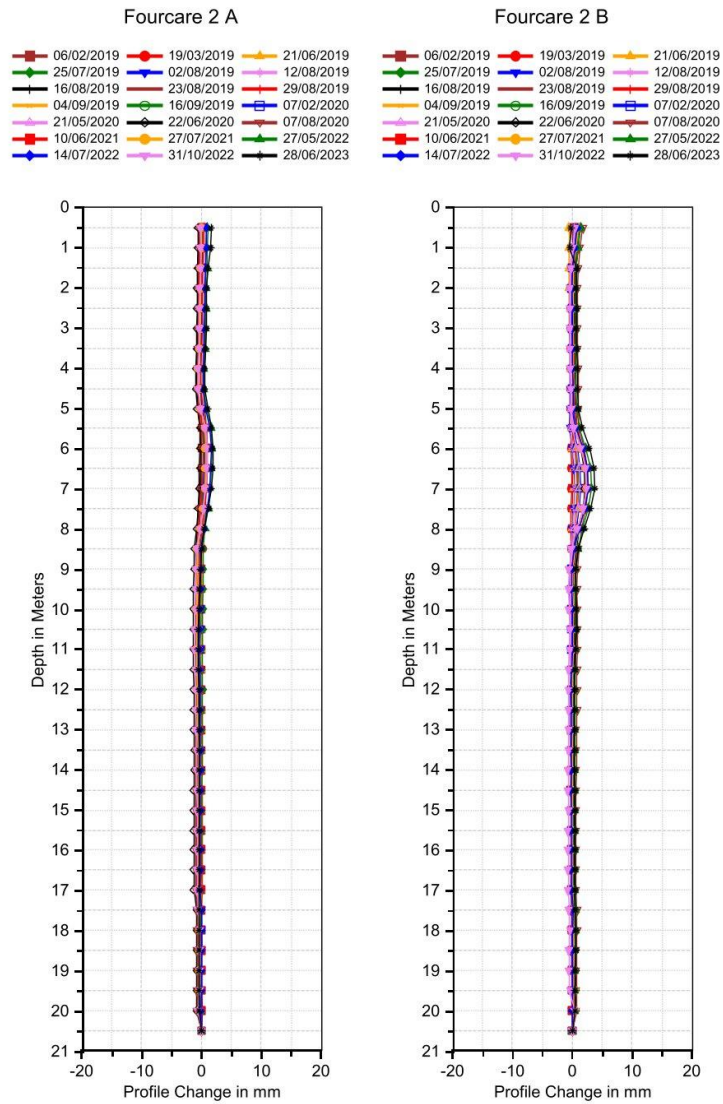
**Figure 8 - shows the displacement profile recorded at the inclinometer number 2 around the Fourcare embankment. It represents the distortion along the primary axis (A) of the probe and the lateral axis (B), which is perpendicular to axis A.**

## Fourcare 3 A

| | | |
|---|---|---|
| 19/03/2019 | 21/06/2019 | 25/07/2019 |
| 02/08/2019 | 12/08/2019 | 16/08/2019 |
| 23/08/2019 | 29/08/2019 | 04/09/2019 |
| 16/09/2019 | 21/05/2020 | 22/06/2020 |
| 07/08/2020 | 10/06/2021 | 27/07/2021 |
| 27/05/2022 | 14/07/2022 | 31/10/2022 |
| 28/06/2023 | | |

## Fourcare 3 B

| | | |
|---|---|---|
| 19/03/2019 | 21/06/2019 | 25/07/2019 |
| 02/08/2019 | 12/08/2019 | 16/08/2019 |
| 23/08/2019 | 29/08/2019 | 04/09/2019 |
| 16/09/2019 | 21/05/2020 | 22/06/2020 |
| 07/08/2020 | 10/06/2021 | 27/07/2021 |
| 27/05/2022 | 14/07/2022 | 31/10/2022 |
| 28/06/2023 | | |
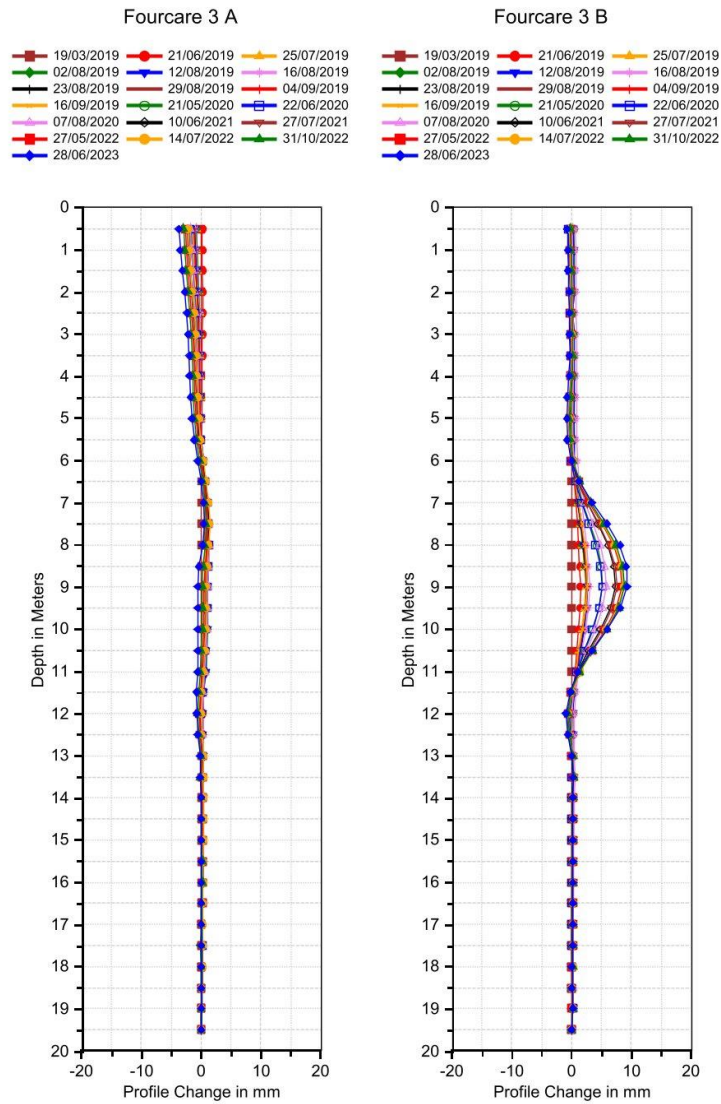
**Figure 9 - shows the displacement profile recorded at the inclinometer around the Fourcare embankment. It represents the distortion along the primary axis (A) of the probe and the lateral axis (B), which is perpendicular to axis A.**
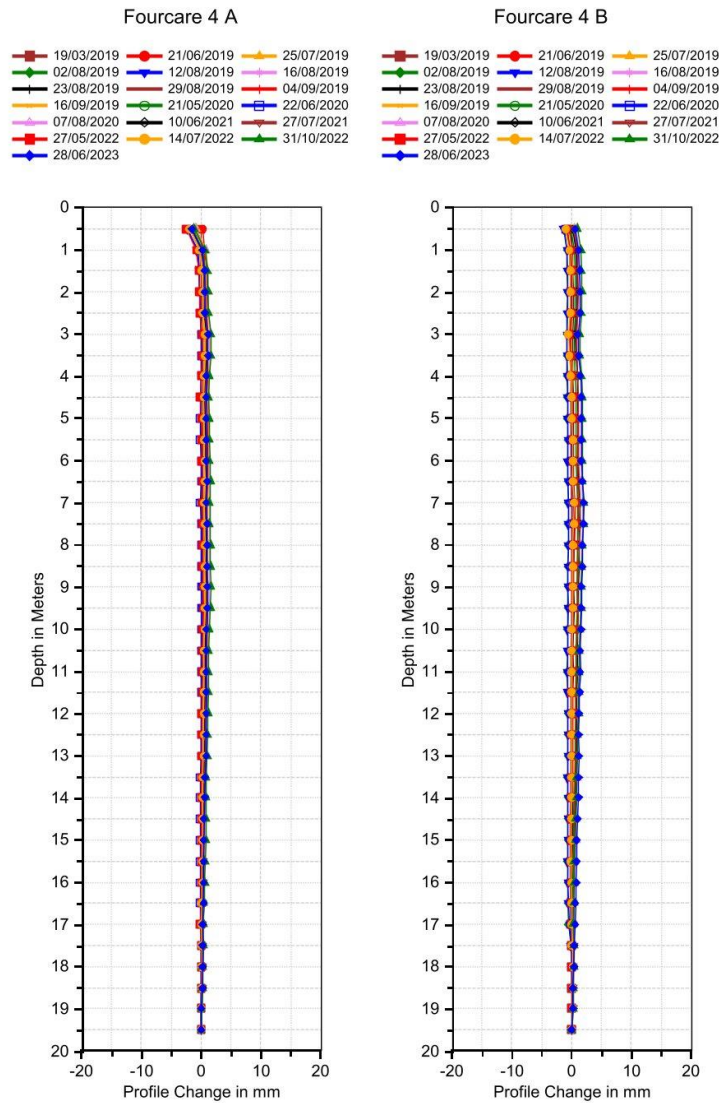
**Figure 10 - shows the displacement profile recorded at the inclinometer number4 around the Fourcare embankment. It represents the distortion along the primary axis (A) of the probe and the lateral axis (B), which is perpendicular to axis A.**

## 2.2 Passive Seismic and Other Methods to Monitor Embankments

The stability, functionality, and safety of embankments are considerably guaranteed by monitoring of their structural integrity. Traditional methods for the early detection of potential risks have been further improved by new technologies. These advancements, including remote sensing, sensor networks, and real-time data analysis, provide more accurate assessments of embankment conditions. The mainly effective methods are summarised below.

### 2.2.1 Automated Monitoring Frameworks

Automated monitoring frameworks are integrated systems designed to continuously monitor the structural health and performance of embankments. These frameworks gather, process, and analyse data in real-time or near real-time, to deliver a complete overview of the actual state of the embankment dams. Through this automation in data collection and processing, early detection of potential issues is facilitated. This possibility enables timely interventions to mitigate risks before they become critical failures. To analyse monitoring data in a faster and more efficient way, automated frameworks have been developed using deep-learning algorithms, such as Long Short-Term Memory networks, which can recognize patterns and detect anomalies in data. These frameworks combine finite element models with real-time monitoring data to come up with more accurate predictions with reduced errors associated with manual inspections (Yang , et al., 2023). The method involves breaking down a large, complex structure or system into smaller, simpler parts called finite elements. Each element is a simple, manageable shape, such as a triangle or square in two dimensions. Each element is connected at nodes, and its behavior is modelled using mathematical equations that take into account material properties and external forces (Yang , et al., 2023).

### 2.2.2 Unmanned Aerial Vehicle Photogrammetry

A dense point cloud model is used for a detailed and accurate analysis of embankment dam deformations, which is generated through Close-range photogrammetry. UAV photogrammetry is currently a very revolutionary resource in monitoring such embankment dams due to their high-resolution data and detailed structural assessments. Unmanned aerial vehicles capture images of the embankment dam surface and further processed them into accurate 3D models with high-resolution cameras, using photogrammetry software. Comparing such models in time allows the engineers to identify small changes in geometry that could be an indication of some structural risks, such as deformation, settlement, or slope instability. This procedure is not too expensive and relatively easy to apply; therefore, it is considered for periodic monitoring of earth and rockfill embankment dams. UAV photogrammetry also serves very well in detection of surface fissures, cracks, or erosion patterns. These anomalies are key indicators of structural wear and points of failure (Wang, Cheng, Xiong, Wang , & Zhao, 2024). In monitoring vegetation growth on embankment slopes, UAV photogrammetry has an essential role. Vegetation growth can cause weakening in structural integrity and increase of seepage risk. As well as mapping the erosion patterns to identify areas that require immediate attention. Additionally, UAV photogrammetry also complements most geophysical monitoring, including GPR and ERT techniques, by providing detailed surface information to enhance the interpretation of subsurface data. Although it is limited in conducting subsurface analysis, the integration of geophysical techniques provides a robust and holistic approach in embankment dam health monitoring for the safety and longevity of critical infrastructure (Chrzanowski & Wilkins , 2007).

### 2.2.3 Electrical Resistivity Tomography

Electrical Resistivity Tomography (ERT) is a geophysical technique of determination of the subsurface resistivity by injection of electrical current into the ground and measure the resulting voltage differences. This method develops high-resolution images of the spatial variations in resistivity, related to material properties such as moisture content and porosity. In particular ERT is effective in seepage detection by identifying areas where the moisture content is increased that can potentially indicate water infiltration or leakage. ERT can also detect internal erosion by identifying areas that resistivity changes due to the saturation of embankment body. Additionally, by mapping heterogeneities and weak zones within the embankment structure, ERT contributes to provide the critical insights into embankment integrity and stability (Sjödahl, Dahlin, & Johansson, 2009).

## 2.2.4 Passive Seismic Methods

Environmental seismology is the study of mechanical vibrations from external sources or environmental changes and anthropogenic activities. The focus of seismic research was primarily on earthquake signals; however, with the advent of continuous waveform data recorded at seismic stations, it has expanded significantly. These data contain signals from a wide range of sources, including those signals generated by environmental processes and human activities. Such signals provide valuable information to the study of Earth's dynamic systems and improving the knowledge of Earth's structure (McNamara & Buland, 2004).

Ambient vibrations, often called ambient seismic noise, can contaminate seismic survey data. These noises cover a wide frequency range include, high-frequency signals (between 1-5 Hz) typically originate from human activities such as industrial operations, machinery, traffic, and low frequency signals below 0.5 Hz, which are typically generated by natural sources. Signals below 0.5 Hz originate from oceanic waves and large-scale meteorological conditions, while the wind and local weather patterns can also generate signals in the 1 to a few Hz ranges (McNamara & Buland, 2004).

Passive seismic methods have become popular for monitoring subsurface conditions because such methods make use of naturally occurring seismic noise and microtremors, with no need for active seismic sources. As they do not require generating artificial seismic waves through explosives or heavy machinery, these methods are cost-effective, non-invasive, and environmentally friendly (de Aguiar & Maciel, 2022).

Passive methods generally require lighter and simpler equipment than active methods and are thus much easier to deploy in remote or difficult to access areas. This allows for long-term continuous monitoring of the data, which is very useful in studying dynamic processes such as changes in structures, subsurface fluid movements or seismic hazards. Embankments are no exception, and the integrity and safety of embankment dams are really tied to a good understanding of subsurface conditions. These passive seismic techniques allow site characterization of the embankment dams, giving insight into the geological and geotechnical properties that are important parameter for design, monitoring, and hazard assessment (de Aguiar & Maciel, 2022).

Passive seismic data processing and acquisition are quite different for various intended uses, while the principal style of acquisition is basically the same. A signal that may be generated by movement within the embankment body, is recorded by seismic recording instrument which is left for a period to record signals. The instruments used can be geophones for shorter recording periods, broadband seismometers, and other adapted sensors such as accelerometers. The processing techniques of passive seismic methods have been split into three groups: seismic horizontal-to-vertical ratio measurements, event detection and characterization, ambient seismic noise cross-correlation (de Aguiar & Maciel, 2022).

- **ASN Spectral Analysis (HVSR) Technique**

The Horizontal-to-Vertical Spectral Ratio (HVSR) method calculating the ratio between the amplitude spectra of the horizontal (East + North) and vertical components of ambient seismic noise recorded at one station. This concept first came up in the study of Nogoshi & Igarashi in 1971; later on, Nakamura made it widely used as a well-established passive seismic technique to evaluate the characteristics of sedimentary deposits in seismic site investigations (Nakamura, 1989). It has broad application in the estimation of the fundamental resonance frequency of a site, which is an important factor in the understanding of how a location might respond to seismic waves (M. Nogoshi & Igarashi, 1970).

The method concerns the ratio between horizontal and vertical components of ambient seismic noise, including microtremors generated both by natural phenomena like wind and ocean waves, and by anthropogenic activity, which generally generates higher frequency noise. In practice, the HVSR method is so defined that whenever constructive interference occurs in seismic waves for subsurface layers, horizontal oscillations are predominantly higher amplitude compared with vertical oscillations. This resonance basically arises due to significant contrast in acoustic impedance between the bedrock and the overlying layer. Thus, the HVSR method contributes to understand the seismic features of any site and assessing its seismic risk (Yamanaka, Takemura, Ishida, & Niwa, 1994).

- **Ambient Seismic Noise Cross Correlation Technique**

Cross-correlation is a statistical method used in seismic studies to find the similarity between two signals. This technique is often applied to ambient seismic noise or seismic waves recorded at two stations. Research has shown that by cross correlating the recordings of ambient seismic noise between two stations, we can estimate the Green's function (Shapiro & Campillo , 2004).

The Green's function describes how seismic waves would travel from a hypothetical point source to a receiver. This process works like simulating a real seismic source and receiver at the two stations. By correlating the signals, we can figure out how the medium between them would respond. In the theoretical framework of cross correlation, we see that a velocity perturbation causes a time shift in the cross correlogram in a homogeneous medium. This time shift is directly related to the velocity change and thus forms the core of seismic interferometry when it comes to imaging the perturbations in velocity. This is useful for imaging subsurface structures and is often a cost-effective alternative to traditional active seismic methods, especially in environments where it can be difficult to deploy active sources. Several studies have shown how cross-correlation can provide high-resolution seismic data, making it incredibly useful for site characterization and subsurface exploration purposes (Shapiro & Campillo , 2004).

To improve the accuracy of velocity change measurements the stretching technique is used. It entails comparing several possible velocity perturbations by filtering the correlograms in narrow frequency bands around a central frequency and then resampling the data to stretch the time axis with respect to a reference correlogram (Larose, et al., 2015). The technique detects small velocity changes in the subsurface and has been found useful in the monitoring of subsurface changes over time. The best velocity change is set as the correlation coefficient between the stretched and reference correlograms. The perturbation that gives the highest correlation is taken as the velocity change. This method has been used effectively in a number of seismic interferometry studies to increase the accuracy of subsurface imaging (Curtis, Gerstoft, Sato, Wapenaar, & Snieder, 2006).

The change in surface wave velocity at a given frequency is mainly attributed to the change in shear wave velocity, while the shear modulus (G) and the density ($\rho$) of the medium control the wave propagation. The depth of investigation is reversed with the frequency band of interest; lower frequencies probe deeper into the subsurface. A decrease in rigidity may be due to processes such as failure and results in a negative irreversible velocity change. Accordingly, seismic noise cross-correlation that is sensitive to small velocity changes can be employed in the early warning systems for monitoring of subsurface instability or seismic (Shapiro & Campillo , 2004).

- **Microseismicity Technique**

A microseismic event is the release of small vibrations. These events are typically caused by small movements in geological formations or by human activities like mining, construction or hydraulic fracturing.  It is possible to sense microseismic events with geophones; moreover, their cumulative events can be quite helpful in the identification of subsurface events and processes and may even reveal potential hazards such as changes in reservoir pressure or fault movement. The causes of microseismic events are mainly mechanical changes in the embankment such as fault movement, settlement or changes in water pressure. It could mean that leaks, cracking and the general weakening of the embankment structure is starting to develop. The events are pick up with the help of equipment that are highly sensitive. These instrumentations are either a set of high-sensitivity triaxial (3C: N, E, V) broadband seismometers or low-frequency geophones (+ digitizer for data acquisition and storage + power supply). Wireless units allow to deploy arrays of sensors even in remote or arduous sites where active seismic prospecting is not feasible and to cover wider areas (Le Calvez & Ay, 2024). In Figure 11 commercial triaxial seismometers from different producers are shown.
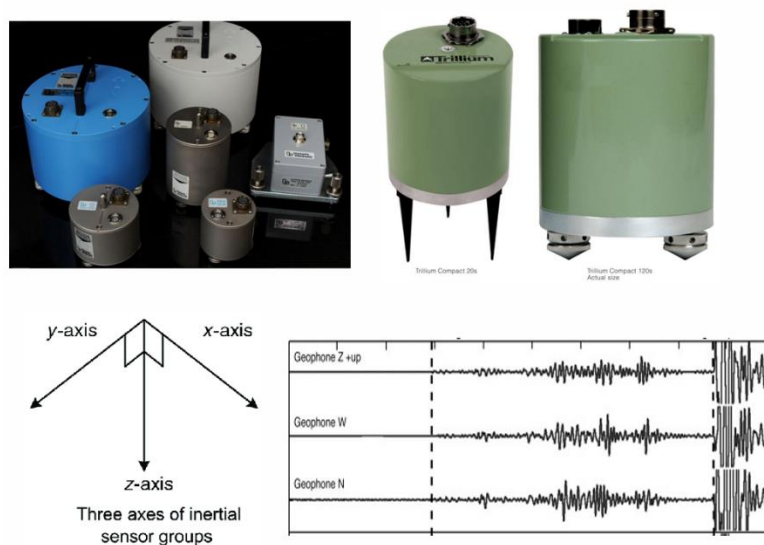


**Figure 11 - top image depicts commercial triaxial seismometers from different companies. The bottom right picture is a sketch of triaxial seismometer measuring velocity along three orthogonal axes, two horizontal (west and north) and one vertical. The bottom-left picture shows an example of a recording from a triaxial seismometer of the vertical, west and north components.**

The data is recorded using a network of seismometer which is installed around the embankment to record ambient seismic noise and microseismic events. These seismometers can be placed at different locations on the surface of the embankments or in the foundations. These events usually are low magnitude and require certain instrumentation and detection techniques. One of the algorithms for detecting such events is the STA/LTA method which is intended to detect small changes in the seismic signals that may represent a microseismic event (Baria, et al., 2004).

The STA/LTA method compares the short time average (STA) and the long time average (LTA) of the amplitude of a seismic signal with time. It is generally used to detect transient events based on the change in seismic amplitude with respect to the background noise to find sudden increases in amplitude. Thus, STA is computed as the average of the signal in a short time window (usually a few seconds), and LTA is computed over a longer period of time (several seconds to minutes) to include the background noise. Then, the algorithm determines the ratio between the short time average and the long time average. When the short time average is considerably higher than the long time average, it exceeds the predefined threshold, so it is suspected to have an event. The STA/LTA ratio is usually used as a trigger to set off an alarm or to define the beginning of an event. This exceedance is usually associated with changes in the embankment dams' structure. The algorithm is useful for real-time monitoring and early detection of small shifts or failures in structures but requires careful calibration to avoid false positives from ambient noise interference (Shapiro & Campillo , 2004).

After the detection of events, events will then be classified. Event classification in seismic monitoring is the process of distinguishing between different types of seismic events by their characteristics of amplitude, frequency and duration. It is important to know whether the seismic signals that have been identified are natural events such as earthquakes or man-made disturbances such as microseismic events caused by infrastructure. Some possible features such as the short time average over long time average ratio, shape of the waveform, the signal arrival time, duration and frequency spectrum of the signal are used criteria to classify the events. However, advanced machine learning techniques are being widely used to automate this process to enhance efficiency and accuracy. Also, signal clustering or pattern recognition algorithms can sort through seismic events and find similarities to help reveal the cause and lead to better early warning systems for monitoring of structural integrity. Seismic events are classified visually based on the frequency

content of the seismic signal using spectrograms (Habbak , Abdalzaher, Othman, & Mansour, 2024).

In visual classification, analysts look at the spectrogram to identify important features including frequency bands, time domain features, or any other pattern that is indicative of an event of interest. A spectrogram is a graphical representation of the frequency contents of a signal as a function of time and is analyzed to determine how the frequency content of the signal is changing with time. It gives a detailed view of frequency content changes with time; therefore, it is a useful tool in distinguishing between different kinds of seismic activity, from microseismic events to earthquakes, and even noise. Visual classification of seismic events using spectrograms means analysing how the frequency content of a seismic signal changes over time. For instance, the seismic signal of an earthquake may show sharp and wide frequency components, while microseismic events are seen as having impulsive, of short duration signals, with triangular envelope, and clear coda (Colombero, 2023).

The microseismic signals are usually manifested by a sharp rise in energy in the spectrogram, which is then followed by a smooth reduction of high frequency content with time. The amplitude of these events can also vary, and in some cases the high frequency components may be missing or partially present. Microseismic events can be single or can be repeated and at certain intervals. The ability to detect and classify these events, especially when they occur in sequences, is important for monitoring structural integrity in environments such as embankment dams where such signals may indicate the need for further investigation such as subsurface movement or fracture (Bensen, et al., 2007).

## 2.3 Workflow

In this study, passive seismic methods are used for the characterization and monitoring at Fourcare Dam. The monitoring was applied at four geophysical stations; however, three of these stations were suffered from tilting during the monitored period. Figure 6 represents the location of each passive seismic stations regarding the Fourcare Embankment. The data from three stations were unusable for further analysis and in particular for performing cross-correlation analysis. Hence, the study aimed at analysing the spectral characteristics of ambient seismic noise and detecting microseismic events.

### 2.3.1 Power Spectral Density Analysis

In this study the Power Spectra Density is computed based on below formula on each hour of available recording for all the three components of East, North, and Vertical at the four passive seismic monitoring stations with the use of MATLAB codes. The Power Spectral Density (PSD) is a statistical measure that describes how power is distributed with respect to frequency in a signal. PSD is simply calculated as the square of the amplitude spectrum, which is the amplitude of each frequency, normalized by the twice of the variation of sampling interval over the number of samples in each segment (McNamara & Boaz, 2006). Figure 12 shows the network spectra with straight line segments fitted to the high noise and low noise.

$$PSD \ = \frac{A^2}{\frac{2\Delta T}{N}}$$

A= Amplitude of the signal

ΔT= sampling interval

N= the number of samples in each segment
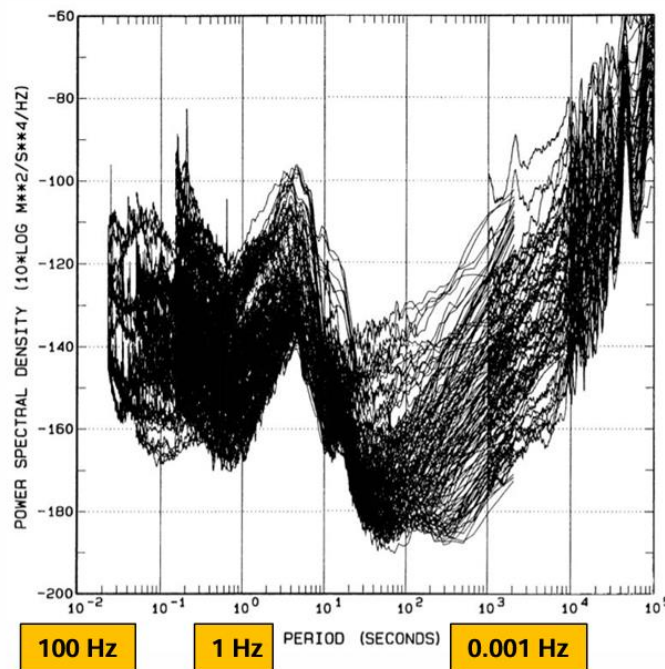
**Figure 12 - shows the network spectra with straight line segments fitted to the high noise and low noise.**

In passive seismic studies, it is necessary to analyse the results of the Power Spectral Density to verify if the ambient noise is within the relevant frequency range. The background seismic noise models, which define the amplitude values for the frequency range from a maximum of 100 Hz down to 0.001 Hz, were created for this purpose. Earth noise models have been available since 1959, when Brune and Oliver released curves of the high and low background seismic noise based on a survey of station noise that was conducted worldwide. This was a benchmark for evaluation of the specifications of the instrument, station site characteristics, and understanding the response of sensor systems to noisy and quite background conditions (Peterson, 1993).

In 1993 Jon Peterson, who analysed noise data from global seismic stations, introduced the new high noise model and new low noise model, which describe the upper and lower limit for the ambient seismic noise. The New Low Noise Model is made of spectra from stations gathered from various instruments, geological environments, and geographic regions which are a hypothetical background

spectrum. The New High Noise Model is the average of high background noise of power in the station network probably it is possible to find nosier sites periods of time that the station might be affected by microseismic storms or by anthropogenic activity disturbances, but the New High Model represent the average value. These models were based on spectral analysis of seismic noise and were adopted as standard references for evaluating seismic station performance and site conditions. In fact, these models are obtained by calculating the Power Spectral Density (PSD) of ambient seismic noise at different locations and then comparing these PSD values to define the thresholds. The new high noise model and new low noise model remain are important for passive seismic monitoring, seismic network design, and assessing effects of environmental seismic data. The ideal level of ambient seismic noise is between high and low noise environments to ensure useful data are provided for further analysis (Peterson, 1993).Figure 13 show the new high and noise model published by Jon Peterson in 1993 by comparing the ambient seismic noise from 75 seismological stations across the earth.
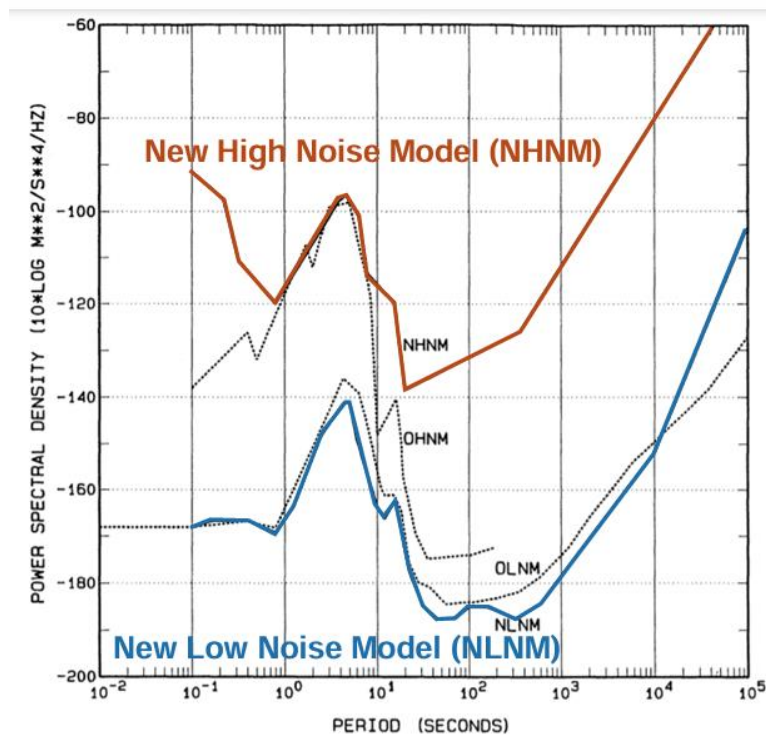


**Figure 13 - show the new high and noise model published by Jon Peterson in 1993 by comparing the ambient seismic noise from 75 seismological stations across the world.**

## 2.3.2 Ambient Seismic Noise Spectral Analysis

A Spectral Analysis of Ambient Seismic Noise is performed following the Power Spectral Density (PSD) analysis, which verified that ambient noise levels are within the accepted range of the Peterson noise model. Moving forward to the next step, Ambient Seismic Noise Spectral Analysis (HVSA) is computed based on the ratio between the amplitude spectra of the horizontal (East+ North) and vertical (V) components of ambient seismic noise at one station. The computation was done in MATLAB on each hour of available recording at the four passive seismic monitoring stations. This ratio is calculated to characterize the resonance frequency of the soft layer, and its accuracy strongly depends on the impedance contrast between the two layers. Then, the frequency domain of the spectral ratio is analyzed to identify the peak in the frequency domain that corresponds to the resonance frequency. Subsequently, we plotted the spectral ratio as a function of time to look for changes in the resonance frequency.

$$F_0 = \frac{Vs}{4H}$$

$F_0$ = resonance frequency

$V_s$= shear wave velocity

H= thickness soft layer
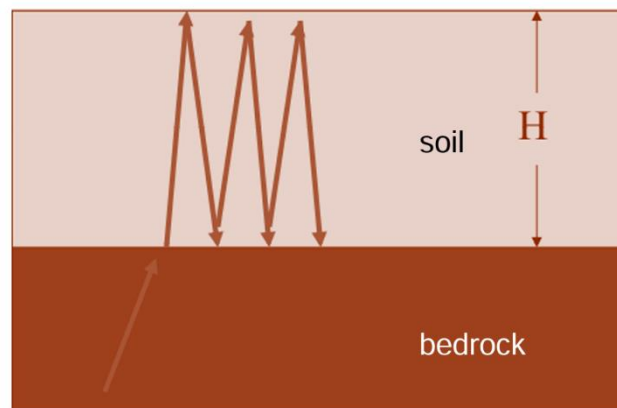


**Figure 14 - shows that whenever there is a soft layer over a hard layer, the acoustic impedance contrast causes the resonance frequency to be trapped in the soft layer.**
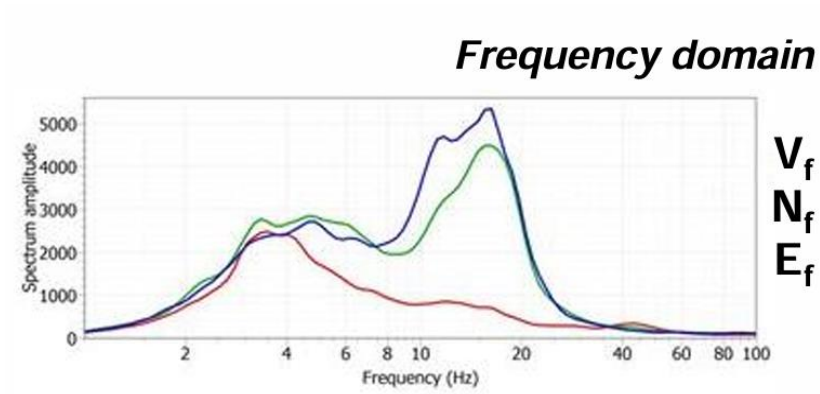
**Figure 15 - shows frequency domain of the spectrum amplitude of a signal for three components of the signal (vertical, north and east).**

$$H_f = \sqrt{E_f^2 + N_f^2}$$

$$HVSR = \frac{H_f}{V_f}$$

**Figure 16 - top equation shows amplitude value of the horizontal component of the signal while the bottom equation calculates the ratio between the amplitude of the horizontal component to the vertical component of the signal.**
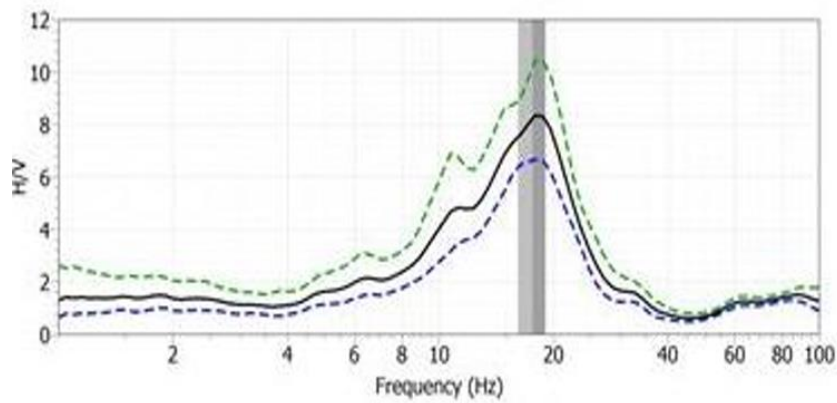


**Figure 17 - shows the horizontal to vertical ratio of the signal over frequency in which we can identify the peak frequency of the signal.**

### 2.3.3 Microseismicity

In this study, microseismic events were detected with the short time average over long time average algorithm and the detected events were classified. Finally, the cumulative number of events and peak frequency of events were plotted. The computation was done in MATLAB on each hour of available recording for the station number 3.
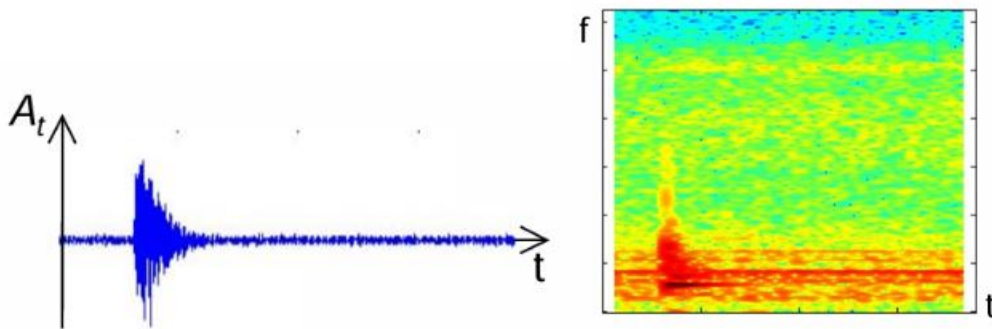


**Figure 18 - right image is an example of the time domain of the amplitude spectrum of a detected event using STA/LTA algorithm. left image is an example of a spectrogram for a detected event.**
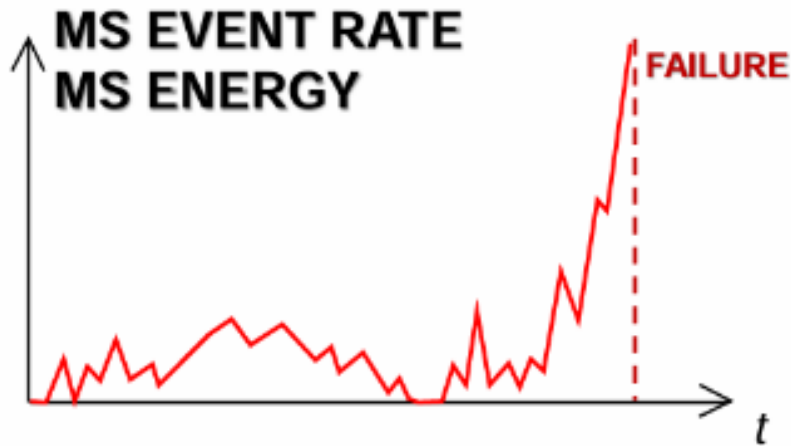


**Figure 19 - shows an example of a plot describing the number of microseismic events over time in which we can see the increase in the number of events is associated with a failure.**

- **Event detection**

    In this study, microseismic events were detected by the Short Time Average (STA) over Long Time Average (LTA) with MATLAB for the station number 3. At a given point, two time windows are selected: a short window (e.g., 1 second) and a long window (e.g., 10 seconds) before the test point. The algorithm calculates the ratio between the average amplitudes (or energy) of the signal on a short time window (STA) and on a long time window (LTA). If the value for the STA/LTA exceeds a predefined threshold, then the event is identified. This detection enables us to classify the events and further analysis.

**If STA/LTA ≥ "threshold" → an event is detected**
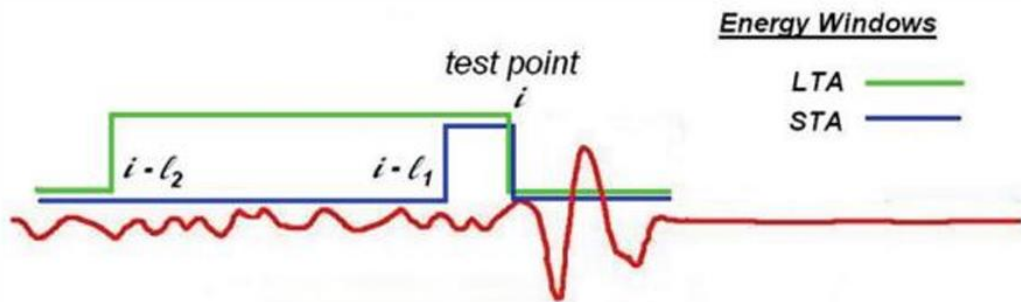


**Figure 20 - shows an example of picking a short and long time windows preceding a point in a signal using the STA/LTA algorithm.**
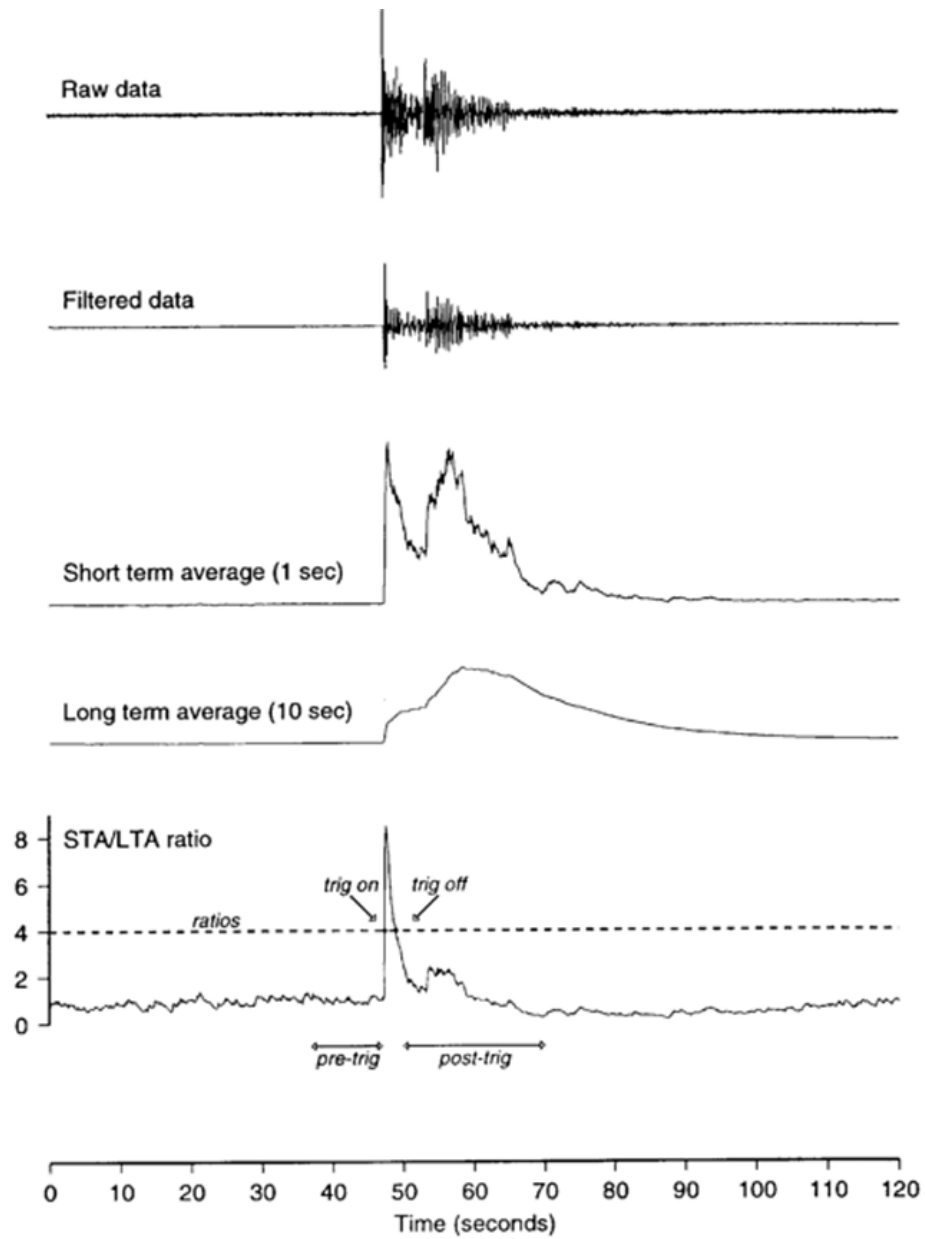
**Figure 21 - shows images illustrating the detailed procedure of STA/LTA algorithm. Top image is the raw data of the signal while the second one is the filtered version of the signal. The two images in the middle illustrate respectively, the short time window and long time window preceding a point in the signal. The bottom image illustrates a time domain plot of the ratio between short time value over long time value in which it can be seen where the ratio is crossing the predefined threshold.**

## • Event Classification

Following the event detection, the classification process was done by visual interpretation. The events were analyzed and compare with reference works from the literature and visually identify a few classes of recurrent events and give an interpretation. The signal was analyzed in time domain (as it was recorded and detected by the STA/LTA algorithm), the amplitude spectrum of the signal, and the spectrogram, which describes the spectrum of frequencies of a signal over time, computed in MATLAB for the station number 3. Microseismic events have a distinct feature to be classified from other events such as noise created by rain drops, human activity on the surface, earthquake and so on. Their maximum amplitude normally in lower frequencies is not specific and varies and even the high frequency is missing. Microseismic events normally are impulsive and short duration which envelope has a triangle shape with a clear coda. The microseismic events spectrogram usually has a sudden energy rise in all frequencies which is followed by an exponential decay of the high frequency with time. They can occur once or in a sequence of events.



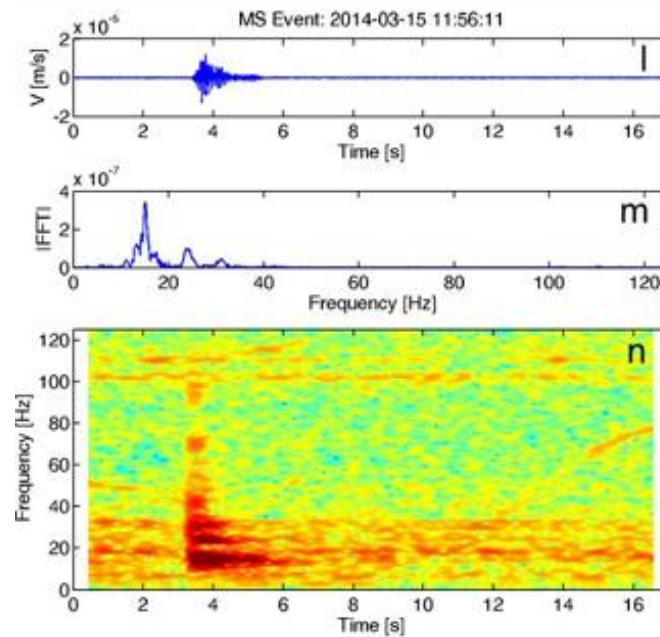**Figure 22 - is an example of a microseismic event with an impulse, short duration signal and a triangular spectrogram shape, where the high frequency content is partially missing.**

- **Cumulative Number of Events**

The cumulative number of events in passive seismic monitoring is the sum of the detected events over time. This is particularly useful in identifying changes, for instance, in the rates of seismicity, which may be indicative of changes in stress state of the subsurface or in fault activity. In hydraulic fracturing or geothermal reservoir stimulation, the cumulative function is used to monitor the propagation of fractures and assess the effectiveness of the treatment, as the total number of events correlates with the extent of the stimulated rock volume. The curve's slope can identify phases of activity, such as fracture saturation, where the rate of new events diminishes, or acceleration that may precede significant seismic events (H.Scholz, 2019). In this study the computation of cumulative number of events was done by MATLAB, and the distribution of events was analyzed and compared with meteorological data for the station number 3.

- **Peak Frequency of Events**

The peak frequency of events is the highest value of each detected events with respect to the time. In this study, the peak frequency of events over time is analysed in the context of microseismicity associated with the embankment, as it can exhibit distinct variations in response to environmental factors such as temperature and precipitation. For example, the aggregation of peak frequencies in the low frequency range over a specific period may indicate the propagation of fractures. Furthermore, Temperature fluctuations can affect the mechanical properties of embankment body, which may be reflected in variations in peak frequency, particularly at lower values. Precipitation, on the other hand, may indicate the saturation of pores and infiltration of water into the embankment structures and potentially trigger seismic events. This can be reflected in the aggregation of peak frequencies in higher values over a specific period. Hence, the relationship between meteorological conditions and the seismic events is often observed by tracing the peak frequency of events over time, which can be a reflection of mechanical properties of embankment body. In this study, the computation was done by MATLAB for the station number 3 for the frequency range between 10 to 50 Hz where the microseismic events mostly were spotted in the spectrogram.

# Chapter 3

# Results

## 3.1 Power Spectral Density Analysis

This section presents the Power Spectral Density (PSD) results for the North, East, and Vertical components recorded at passive seismic monitoring station 3 of the Fourcare embankment. The analysis indicates that the ambient seismic noise observed during the study falls within the defined limits of Peterson's New Low Noise Model (NLNM) and New High Noise Model (NHNM). Noise levels within this range ensure that the recorded seismic signals are not excessively influenced by environmental disturbances.
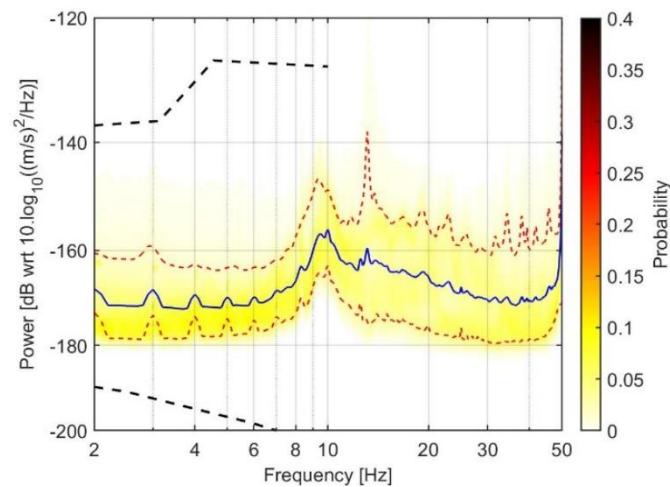


**Figure 23 - Shows the power spectral density of the east component at passive seismic station number 3, for the Fourcare Embankment.**
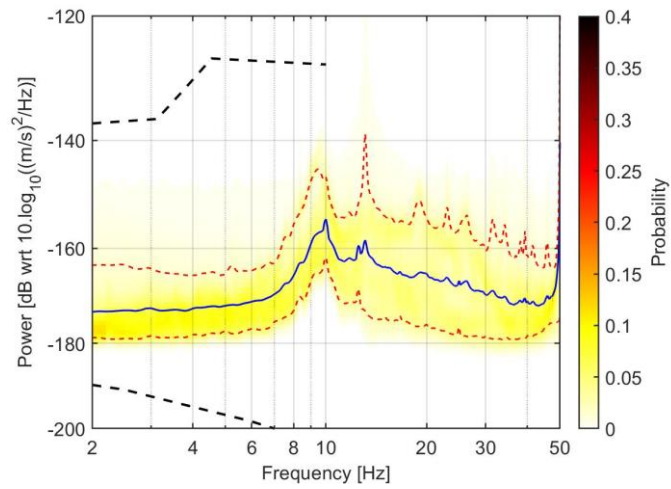
**Figure 24 - shows the power spectral density of the north component at passive seismic station number 3 , for the Fourcare Embankment.**
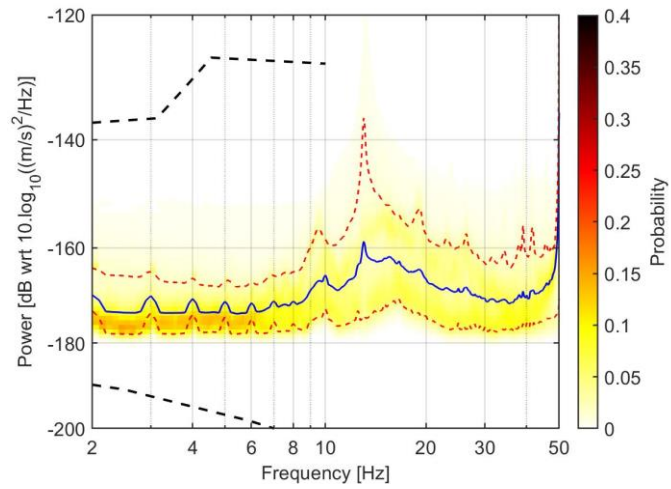


**Figure 25 - shows the power spectral density of the vertical component at passive seismic station number 3, for the Fourcare Embankment.**

# 3.2 Ambient Seismic Noise Spectral Analysis

**Frequency Domain of The Horizontal to Vertical Spectral Ratio**

In this section the result of the frequency and time domain of the Horizontal to Vertical Spectral Ratio recorded at the passive seismic station number 3 of the Fourcare embankment is depicted. Figure 26 illustrates the frequency domain of the Horizontal-to-Vertical Spectral Ratio (HVSR) results applied at the passive seismic station number 3 of the Fourcare embankment.

The peak in the H/V spectrum can be served as an indicator of the resonance frequency of the embankment. The results highlight the resonance frequency of the site at around 10 Hz. This value reflects the subsurface characteristics, material properties and geometry of the embankment. The resonance frequency of 10 Hz corresponds to the fundamental vibration mode of the site, influenced by factors such as the thickness and material properties of the layers. This parameter is critical for assessing the site's seismic response and potential vulnerabilities, providing valuable insights into the local geological conditions.

**Time Domain of the Horizontal to Vertical Spectral Ratio**

Figure 27 shows time domain of the Horizontal to Vertical Spectral Ratio of the station 3. According to the result of H/V over time the resonance frequency is almost stable at 10 Hz over time, except a period of November and December of 2023 that the frequency is sort of disturbed mainly because of the reduction of temperature and freezing the embankment body. This indicates that despite environmental changes the embankment structure and subsurface layers are relatively not affected by short-term variations in temperature and precipitation.
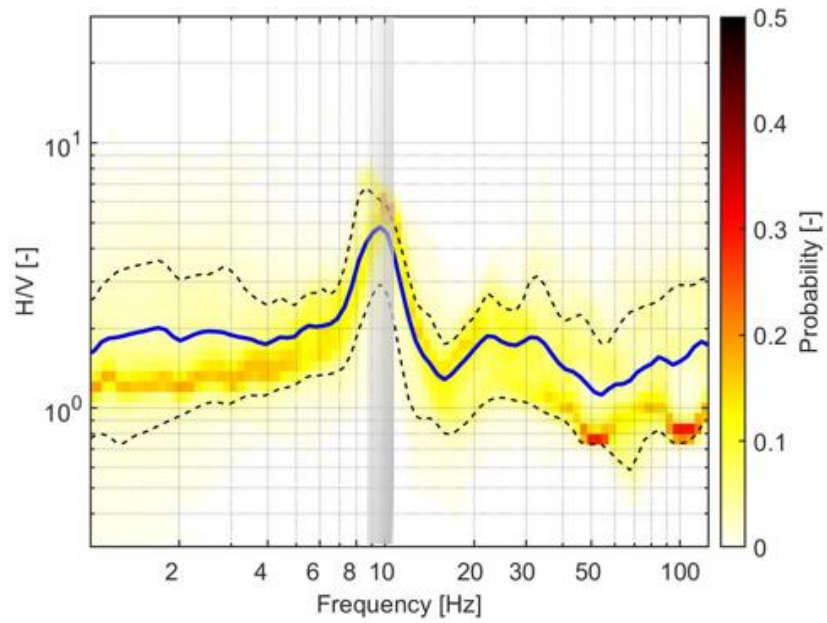
**Figure 26 - shows the frequency domain of the horizontal-to-vertical spectral ratio (H/V) applied at passive seismic station number 3 of the Fourcare Embankment.**
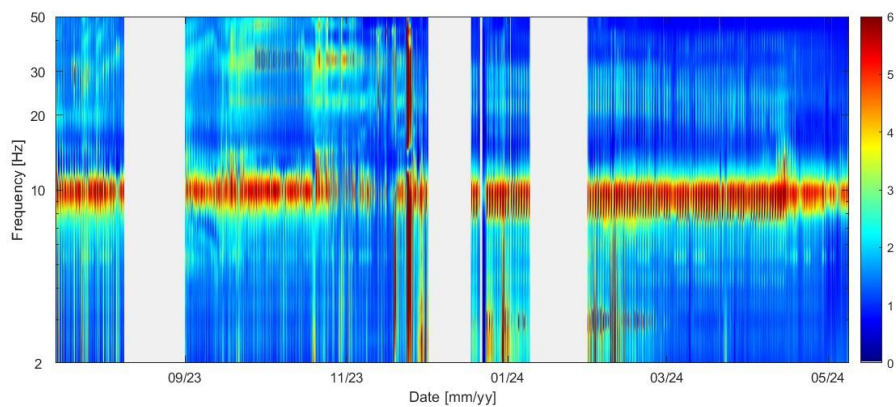


**Figure 27 - shows the horizontal-to-vertical spectral ratio (H/V) over time at passive seismic monitoring station number 3, covering the period from August 2023 to May 2024 of the Fourcare Embankment.**

## Spectral Analysis as a response to meteorological variation Applied at Station Number3

During colder months when temperatures are below zero degrees of Celsius, there are changes in the peaks of the HVSR curves which can be due to changes in the mechanical properties of the embankment materials likely due to freezing. However, these changes are minor which can suggest the embankment structures are relatively stable over time.

In the top graph of Figure 28, the precipitation from the nearest meteorological satiation is shown in the brown spikes. Precipitation makes the embankment structure saturated which can have an impact on the impedance contrast between the two layers and subsequently disturbance in the resonance frequency. This effect can exacerbate in the colder month when the temperature drop. The combination of temperature drop and precipitation in November leads to an unclear in resonance frequency. This emphasized the need to consider the environmental effects on HVSR results in order to evaluate both the short term and long term stability of the embankment structure.
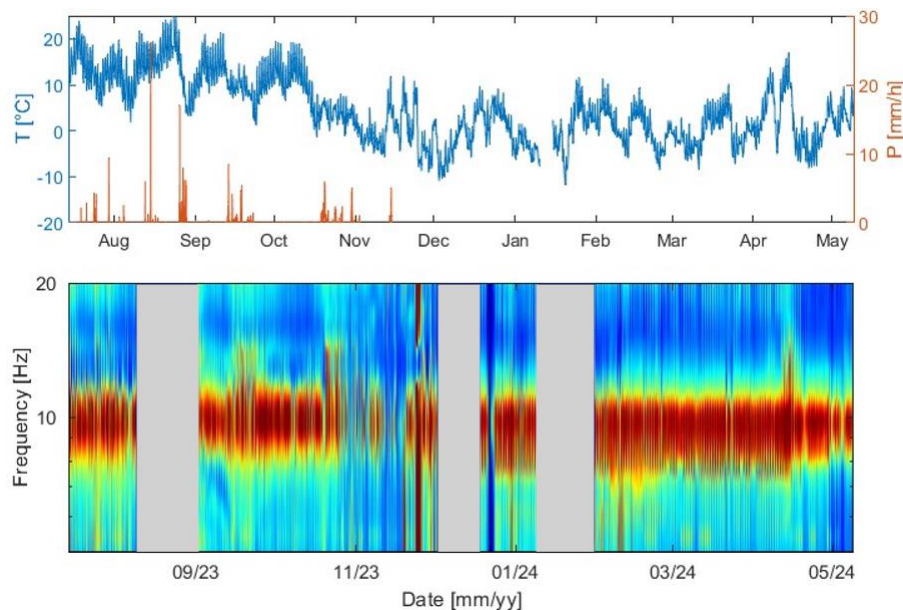


**Figure 28 – consists of two graphs. The top graph shows the temperature and precipitation data from July 2023 to May 2024 of the meteorological station near the Fourcare Embankment. The second graph illustrates the horizontal to vertical spectral ratio over time at passive seismic monitoring station number 3 from July 2023 to May 2024.**
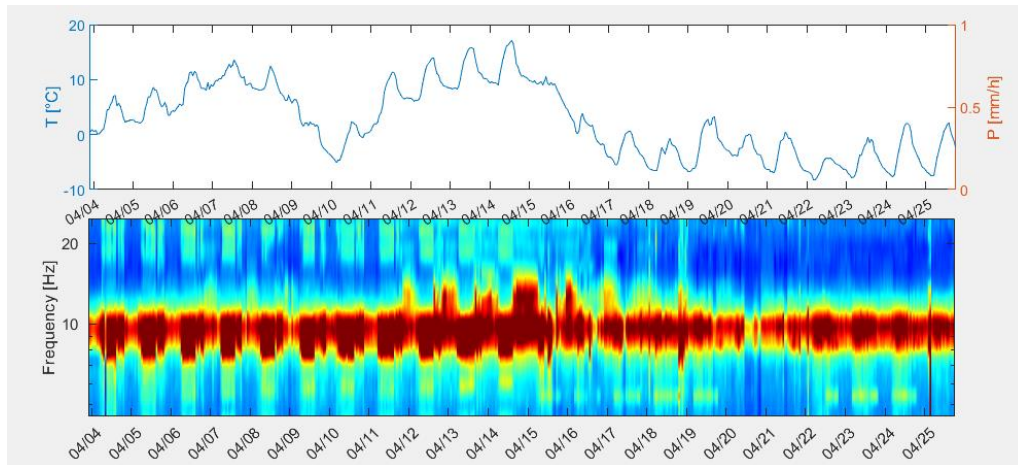
**Figure 29 - shows a zoomed-in period in which we can see that at short term scale, there is stronger resonance frequency when the temperature is high, while a decrease in temperature correspond to a lower amplitude.**
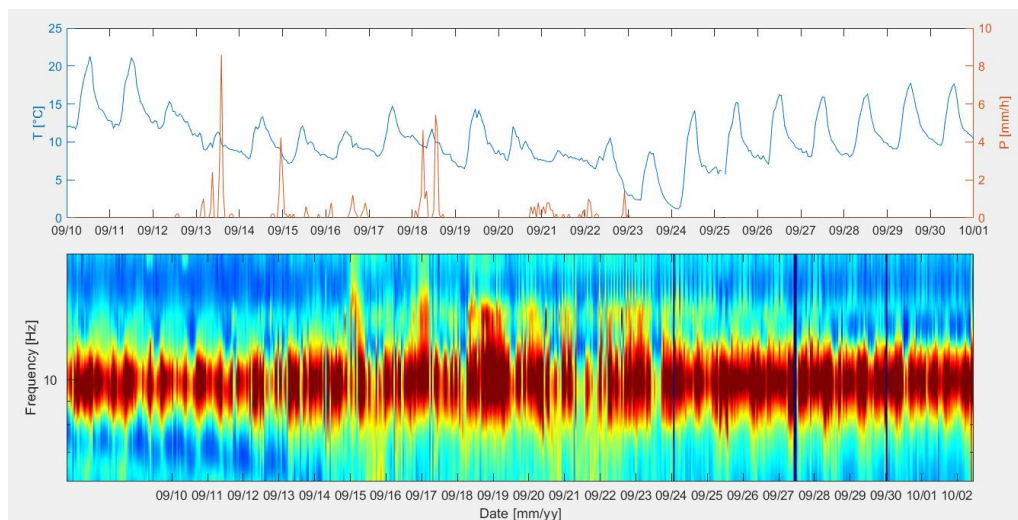


**Figure 30 - shows a zoomed-in period in which we can see that, at the daily time scale, there is the effect of precipitation on the resonance frequency. The peak of resonance frequency is not narrow and clear during precipitation and there is a perturbation in the resonance frequency due to precipitation.**

**Figure 31 - shows a zoomed-in period in which we can see that whenever there is precipitation, the peak of resonance frequency is not so clear and there are lots of disturbances when the temperature is low.**



**Figure 32 - shows the loss of peak frequency at the resonance frequency at passive seismic monitoring station 3 during November and December 2023, potentially due to a reduction in the temperature and freezing.**

## 3.3 Microseismicity

### 3.3.1 Event Detection and Classification

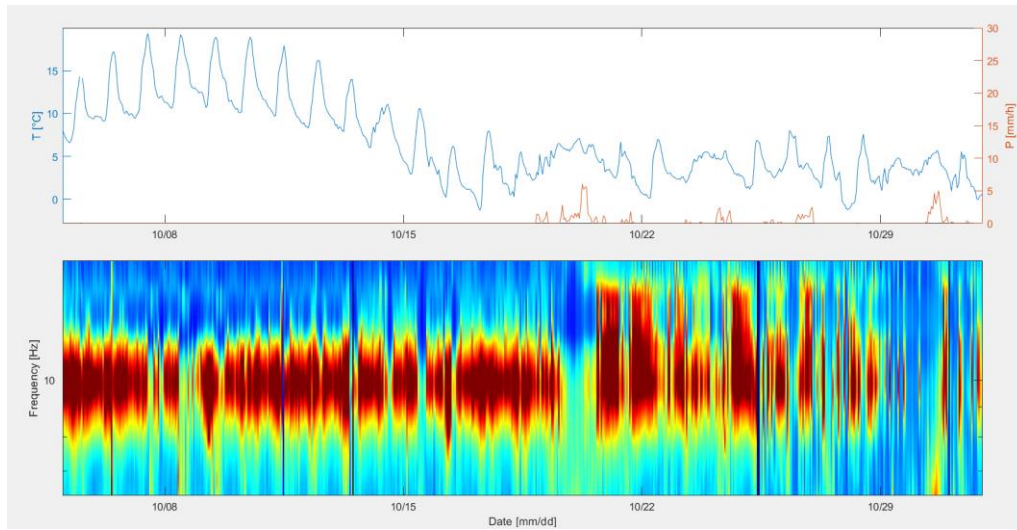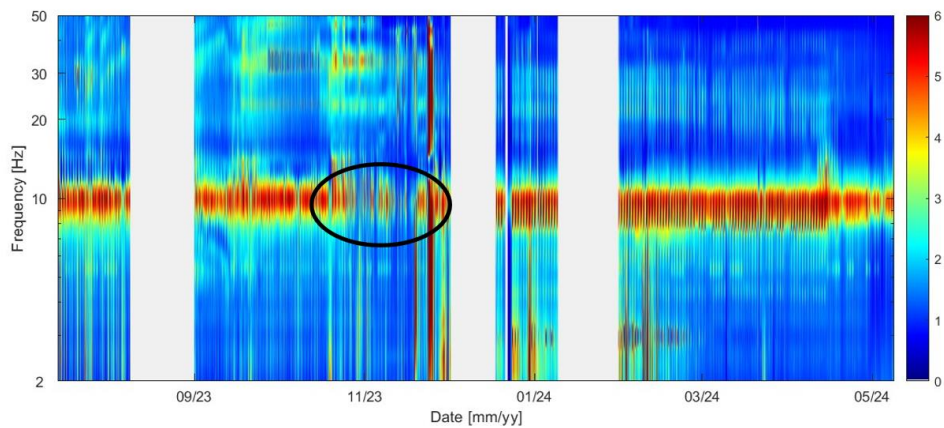In this study, seismic events were successfully detected by STA/LTA (Short Time Average/Long Time Average) algorithm using MATLAB codes for the station number 3. In this section by visual interpretation and comparison with reference works three main classes of seismic events were identified. In the low frequency band, two main classes are identified while there are many events in high frequency band and class three are chosen among them. We are more interested in the low frequency events; that are lower 20 Hz. These events are in two different classes in a very high number. The first class show quite a long duration around a few seconds with a horizontal signature in the spectrograms due to their long duration. Based on their spectrogram they might be related to the weak sliding of the embankment material likely related to the water infiltration. In the same frequency band, there is a second class of events that shows the same peak frequency close to 10 to 15 Hz but shorter duration. This second class has sort of triangular shape in the spectrogram that is diagnostic for fracturing events. So, in the frequency bands below 20 Hz classes, we have almost all the events of interest, material which is associated with microseismic events relate to the fracturing as well as percolation of water which creates some sliding of the materials. Nevertheless, many microseismic events occur in high frequency band. One of the classes, with fewer number respects to the others is characterized by high frequency microseismic events with longer duration, potentially linked to the processes occurring in very shallow layers. It seems that they increase only during the frizzing time, so they likely correlate to the freezing of the material or snow compaction at the site. They are not so useful for the monitoring with lower number in summer period and higher number during winter.

The events that should be followed over time in order to have an interpretation about the micro seismicity of the site all belong to the class of low frequency bands. Hence, further classification is needed to automatically recognize the short duration events which are related to the fracturing from the long duration ones that are likely related to water infiltration or shallow modification.
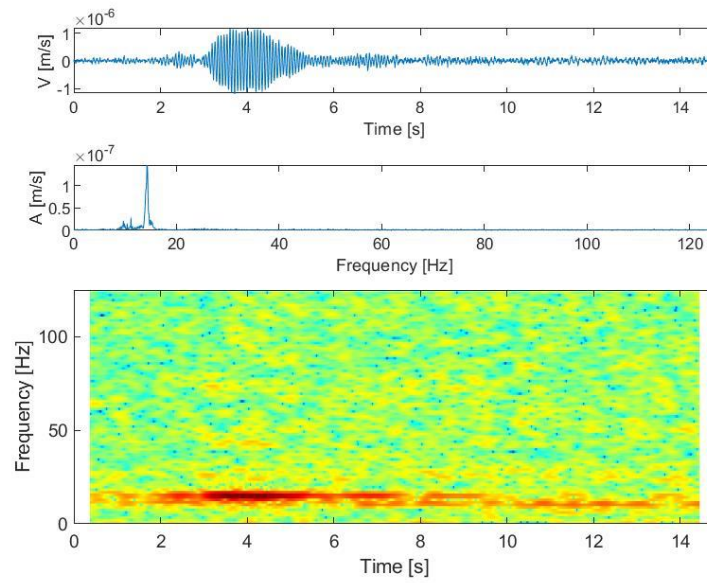
**Figure 33 - shows examples of the first class identified from detected events. This class has distinctive characteristics such as low frequency with a peak frequency ranging from 10 to 20 Hz; moreover, they have quite long durations close to 5 seconds. Additionally, they last for longer time in spectrogram.  These low frequency events might be related to sliding due to water infiltration.**
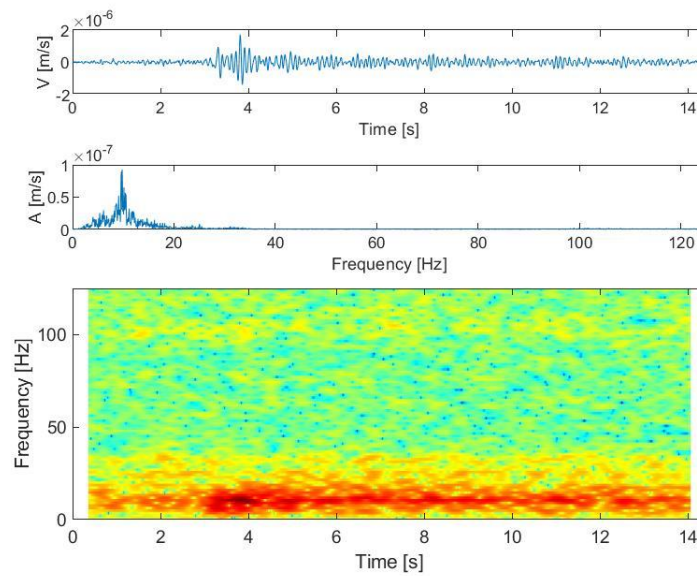


**Figure 34 - shows another example of the first class characterized by a peak at low frequency and longer duration.**
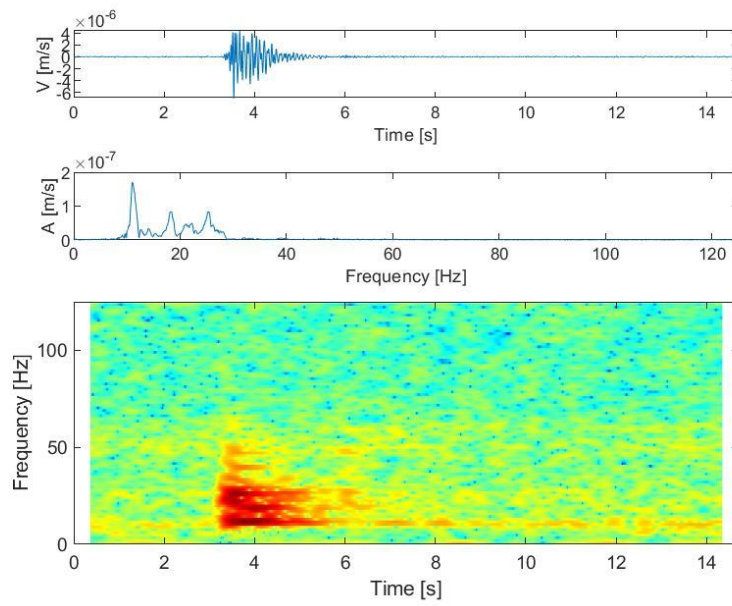
**Figure 35 - shows another example of low frequency events with a peak frequency close to 10 Hz and short duration with a triangular spectrogram. These events might be related to fracturing and weakening of the embankment material.**
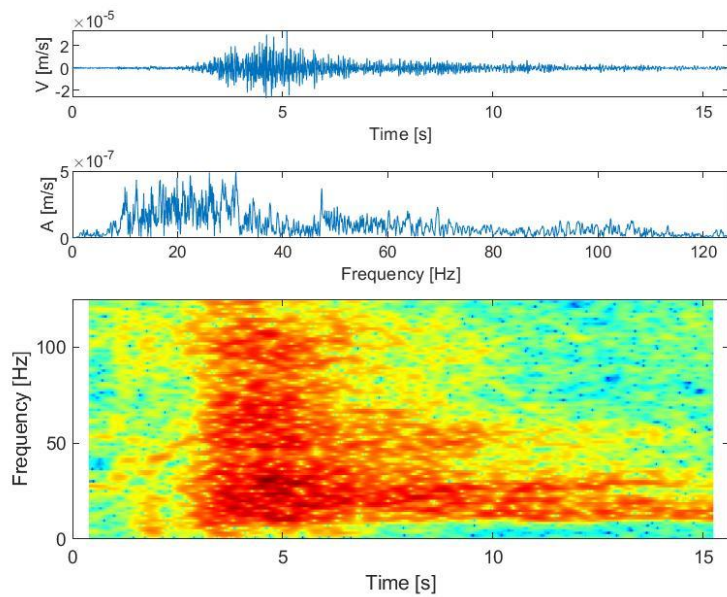


**Figure 36 - shows another example of the second class characterized by peak at low frequency and short duration.**
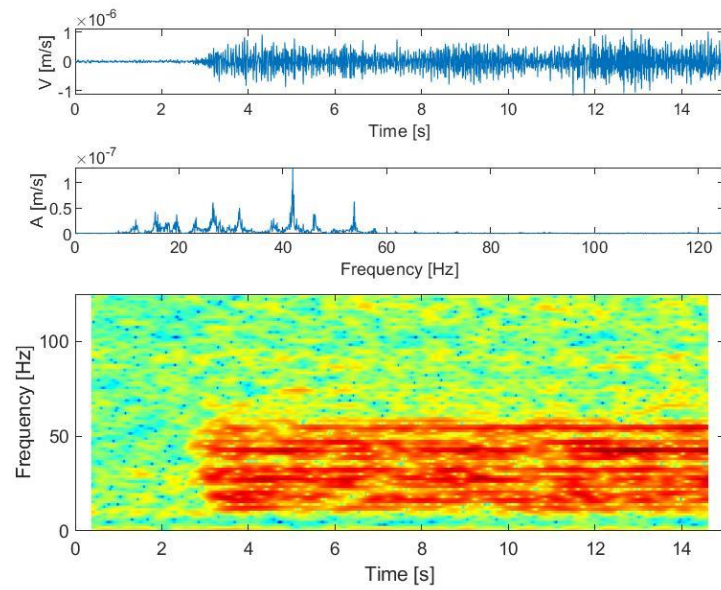
**Figure 37 - shows examples of the third class, characterized by a peak at high frequency close to 40 Hz and a longer duration, ranging from a few seconds to tens of seconds. These microseismic events, which increase in number during the winter period are potentially related to the freezing of the embankment or snow compaction. These events generally occurs in shallower layers.**
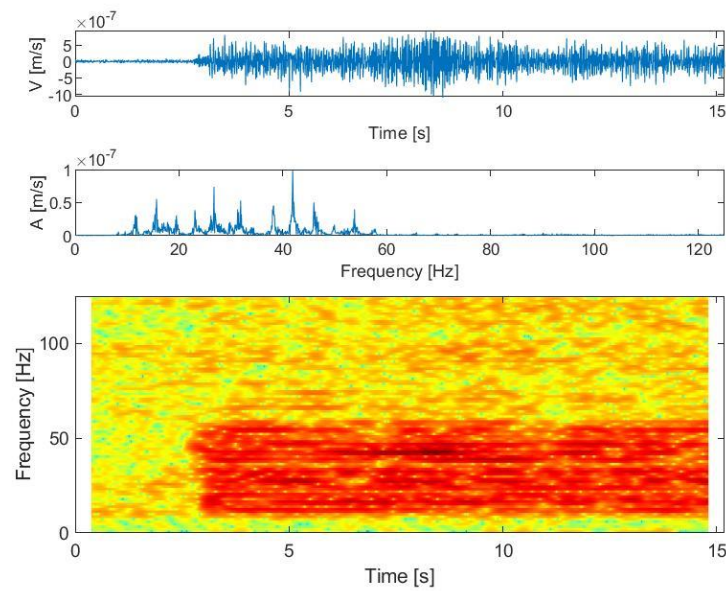


**Figure 38 - shows another example of class three, characterized by a peak at high frequency and longer duration.**

### 3.3.2 Cumulative Number of Events

After event classification, the cumulative number of events was analysed, revealing a sudden increase in both high and low frequency events starting in October. Notably, the low-frequency events exhibited a longer duration and last until the November. In Figure 39 the cumulative number of events are shown. As we can see, there is a slight increase in the number of events associated with both low and high frequencies which may reflect the influence of precipitation on event occurrence. Since early August until September the data related to the cumulative number of events are missing, likely due to technical issues with the seismometer. From September onwards there is a slight increase in the number of microseismic events until October that there is a dramatic rise in the number of microseismic events especially for low frequency events. This rise in the number of events potentially can correspond to the drop in Temperature. Seasonal cooling likely induces thermal stress, which can trigger low-frequency events associated with deeper subsurface processes and development of fractures.
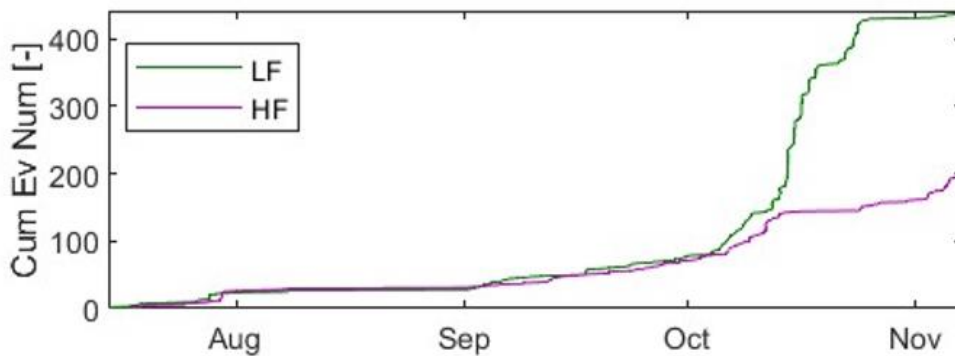


**Figure 39 - shows the cumulative number of microseismic events detected at passive seismic monitoring station number 3.**

### 3.3.3 Peak Frequency of Events

In this section the scatter plot of the peak frequency of detected events at passive seismic monitoring station number 3 from July to November 2023 is depicted. Additionally, the temperature and precipitation data of the nearest meteorological station to the Fourcare embankment are provided in order to have an insight into the response of microseismic events to the changes in temperature and precipitation. In the middle graph of the Figure 40, we can see that the microseismic events are mainly scattered around two distinct frequencies. There is an aggregation of peak frequency at lower value approximately 10 Hz as well as an aggregation of peak frequency at higher frequency around 40 Hz. As temperature drops in October, it can be seen that the concentration of peak frequency of 10 Hz is drastically increase, indicating a rise in the number of micro seismic events in deeper layers. This can be the result of freezing of the embankment body and change in the mechanical properties of the structure. While there is, also increase in higher frequency starting from the October that can indicate the increase in the number of microseismic events in the shallower layers of the embankment.
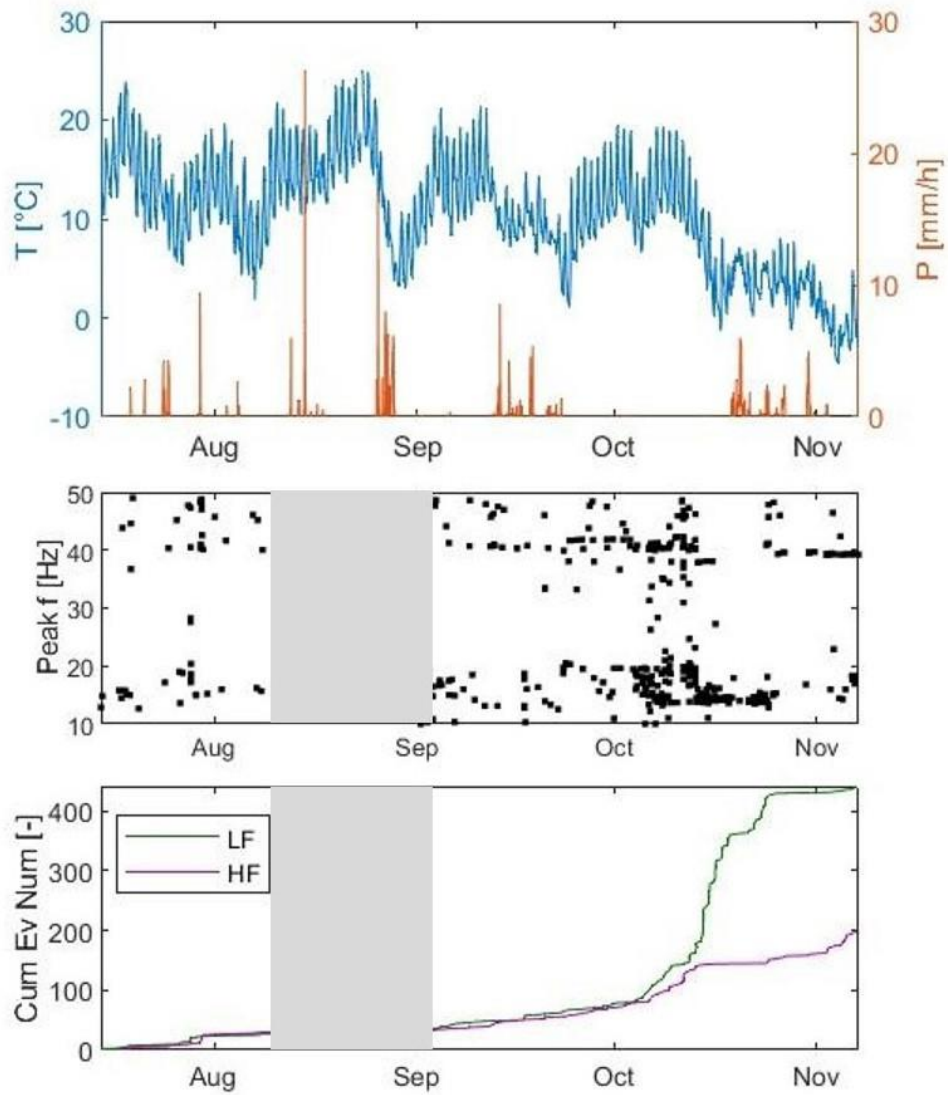
**Figure 40 - consists of three graphs; the top graph shows the temperature and precipitation data from the meteorological station close to the Fourcare Embankment. The middle graph depicts the peak frequency of detected events recorded at passive seismic monitoring station number 3 and the bottom graph is the representation of the cumulative number of events recorded at passive seismic monitoring station number 3 of Fourcare Embankment.**

# Chapter 4

# Conclusion

This study has investigated the application of passive seismic methods for the characterization as well as continuous monitoring of an earthen embankment in the Alpine region in North-west of Italy. Based on the results of inclinometer and piezometers, it was decided to put the four passive seismic monitoring stations in the northern section of the site in which deformation was identified. This study makes an important contribution to the assessment of the stability and integrity of the man-made embankment since there are fewer numbers of studies done with passive seismic in these structures. The findings of the study identified the resonance frequency of the site close to 10 Hz which is stable over time, indicating there are no irreversible modifications in the general stability of the embankment over the monitoring period. However, the findings of microseismic events needs more challenging interpretation. We were able to discriminate the event of our interest which is inside the low frequency classes, lower than 20 Hz. Hence, further classification is needed to automatically recognize the short duration events which are related to the fracturing from the long duration ones that are likely related to water infiltration or modification in shallow layers, as well as analysing their revolution over time for a complete monitoring and warning of the embankment. One limits of the study was performing analysis only for the station number 3 since data from the other three passive seismic stations was missing, so one future suggestion is to obtain the data from the other period of time that are not suffering from the tilt in the passive seismic stations in order to be able to conduct further analysis such as cross-correlation. This study also is limited to a shorter period of time; nevertheless, the findings of this study shows that the monitoring can be ongoing, and a complete analysis of monitoring data can provide a clearer understanding of the embankment integrity and early warning of early detection of irreversible modifications in the stability of the site.

# References

Baria, R., Michelet1, S., Baumgaertner, J., Dyer, B., Gerard, A., Nicholls, J., . . . Megel, T. (2004). Microseismic monitoring of the world's largest potential HDR reservoir. *National Institute of Advanced Industrial Science and Technology (AIST) Tsukuba, Japan*.

Bensen, G., Ritzwoller, M., Barmin, M., Levshin, A., Lin, F., Moschetti, M., . . . Yang, Y. (2007). Processing seismic ambient noise data to obtain reliable broad-band surface wave dispersion measurements. *Geophysical Journal International*, 1239–1260.

Berberan, A., Ferreira†, I., Portela, E., Oliveira, S., Oliveira, A., & Baptista, B. (2011). Overview on terrestrial laser scanning as a tool for dam surveillance. *International Conference on Dam Engineering*.

Bormann, P., & Wielandt, E. (2013). Seismic Signals and Noise. *New manual of seismological* , 62.

Bunton, D. (2002). Generic moves in PhD thesis introductions. In J. Flowerdew, *Academic discourse* (p. 57-75). London: Pearson Education Limited.

Chrzanowski, A., & Wilkins , R. (2007). Fully Automatic and Reliable Real Time Monitoring Systems for Steep Slopes, Embankments, and Structures. *Computer Applications In Geotechnical Engineering*.

Colombero, C. (2023). Passive Seismic for Climate Change Monitoring, Adaotation, and Mitigation. *Slides of the Innovation Lab*.

Curtis, A., Gerstoft, P., Sato, H., Wapenaar, K., & Snieder, R. (2006). Seismic interferometry—turning noise into signal. *The Leading Edge*, 1082-1092.

de Aguiar, G., & Maciel, S. (2022). Earthen Dam Monitoring Using Passive Seismic: A Forward Modeling Study. *Brazilian Journal of Geophysics*.

Fantilli, A., De Biagi, V., Veylon , G., & Frigo, B. (2017). A protocol to assess the seismic criticality of existing small concrete dams. *Structure and Infrastructure Engineering*, 1197-1206.

Foster, M., Fell, R., & Spannagle, M. (2000). The statistics of embankment dam failures and accidents. *Canadian Geotechnical Journal*.

H.Scholz, C. (2019). *The Mechanics of Earthquakes and Faulting.* Cambridge University Press.

Habbak , E., Abdalzaher, M., Othman, A., & Mansour, H. (2024). Enhancing the classification of seismic events with supervised machine learning and feature importance. *Scientific Reports* .

K. Brewitt, P., & L. M. Colwyn, C. (2019). Little dams, big problems: The legal and policy issues of non-jurisdictional dams.

Kanako Taku. (2023). *Earth Dams*, 190-217.

Kwan, B. S. (2009). Reading in preparation for writing a PhD thesis: Case studies of experiences. *Journal of English for Academic Purposes*, pages 180-191.

Larose, E., Carrière, S., Voisin, C., Bottelin, P., Baillet, L., Guéguen, P., . . . Massey, C. (2015). Environmental seismology: What can we learn on earth surface processes with ambient noise? *Journal of Applied Geophysics*, 62-74.

Le Calvez, J., & Ay, E. (2024). Introduction to this special section: Microseismic monitoring. *The Leading Edge*.

M. Nogoshi, M., & Igarashi, T. (1970). On the Propagation Characteristics of Microtremor. *Journal of the Seismological Society of Japan*, 234-264.

McNamara, D., & Boaz, R. (2006). Seismic Noise Analysis System Using Power Spectral Density Probability Density Functions.

McNamara, D., & Buland, R. (2004). Ambient Noise Levels in the Continental United States. *Bulletin of the Seismological Society of America*, 1517-1527.

Morden, R., Horne, A., Bond, N., Nathan, R., & Olden, J. (2022). Small Artificial Impoundments Have Big Implications for Hydrology and Freshwater Biodiversity. *Frontiers in Ecology and the Environment*, 141/146.

Nakamura, Y. (1989). A Method for Dynamic Characteristics Estimation of Subsurface using Microtremor on the Ground Surface. *Quarterly Report of Railway Technical Research Institute (RTRI)*, 25-33.

Ozelim, L., Borges, L., Chaves, L., Araújo, A., Doria, D., Guedes, G., . . . de Aquino, F. (2022). Structural Health Monitoring of Dams Based on Acoustic Monitoring, Deep Neural Networks, Fuzzy Logic and a CUSUM Control Algorithm.

Peterson, J. (1993). Observations and modeling of seismic background noise. *Seismological Research Letters*, 94.

Regis Neroni, Kevin Stephens, & Daniel Dwumfour. (2019). Application of the passive seismic Horizontal-to-Vertical Spectral Ratio (HVSR) technique for embankment integrity. 1-6.

Rixen, C., Teich, M., Lardelli, C., Gallati, D., Pohl, M., Pütz, M., & Bebi, P. (2011). Winter Tourism and Climate Change in the Alps. *Mountain Research and Development*, 229-236.

Ruiz-Armenteros, A., Ruiz-Constán, A., Lazecky, M., Bakoň, M., Delgado-Blasco, J., Sousa, J., . . . Perissin, D. (2022). Monitoring critical infrastructure and anthropogenic hazards in Malaga province (southern Spain) using SAR remote sensing. *EGU General Assembly*.

Shapiro , & Campillo . (2004). Emergence of broadband Rayleigh waves from correlations of the ambient seismic noise. *Geophysical Research Letters*.

Singh, R. (2023). Earthen Embankments and Farm Ponds. In *Soil and Water Conservation Structures Design* (p. 323-366).

Sjödahl, P., Dahlin, T., & Johansson, S. (2009). Embankment dam seepage evaluation from resistivity monitoring data. *Near Surface Geophysics* .

Steiger, R., & Mayer, M. (2008). Snowmaking and Climate Change. *Mountain Research and Development*, 292-298.

Thomas, J., Klida, R., Oommen, T., Sajinkumar KS, Zhang, B., & Hu, X. (2024). Need for a Multi-Sensor Monitoring Approach for Embankment Failures: Lessons Learned from the Edenville Dam Failure. *Environmental & Engineering Geoscience* , 19-30.

United States Bureau of Reclamation. (1987). *Design of Small Dams.*

Wang, K., Cheng, Y., Xiong, Y., Wang , Q., & Zhao, M. (2024). Methods and research for deformation monitoring of earth and rock dams based on close-range photogrammetry. *Measurement Science and Technology*.

Whiteley, J., Chambers, J., Uhlemann, S., Wilkinson, P., & Kendall, J. (2018). Geophysical Monitoring of Moisture-Induced Landslides.

Wielandt, E. (2004). Seismic sensors and recordings [Workshop presentation]. *Institute of Geophysics, Stuttgart University*.

Yamanaka, H., Takemura, M., Ishida, H., & Niwa, M. (1994). Characteristics of long-period microtremors and their applicability in exploration of deep sedimentary layers. *Bulletin of the Seismological Society of America* , 1831-1841.

Yang , C., Chaoning , L., Tongchun , L., Huijun , Q., Dongming , L., & andSiyu , C. (2023). An Automated Framework for the Health Monitoring of Dams Using Deep Learning Algorithms and Numerical Methods.